

# Transistor Circuits For A MEMS Based Transceiver

*Kelvin Liang*



Electrical Engineering and Computer Sciences  
University of California at Berkeley

Technical Report No. UCB/EECS-2015-48

<http://www.eecs.berkeley.edu/Pubs/TechRpts/2015/EECS-2015-48.html>

May 7, 2015

Copyright © 2015, by the author(s).  
All rights reserved.

Permission to make digital or hard copies of all or part of this work for personal or classroom use is granted without fee provided that copies are not made or distributed for profit or commercial advantage and that copies bear this notice and the full citation on the first page. To copy otherwise, to republish, to post on servers or to redistribute to lists, requires prior specific permission.

University of California, Berkeley College of Engineering  
**MASTER OF ENGINEERING - SPRING 2015**

**Electrical Engineering and Computer Science**

**Integrated Circuits**

**Transistor Circuits for a MEMS Based Transceiver**

**Kelvin Liang**

This **Masters Project Paper** fulfills the Master of Engineering degree requirement.

Approved by:

1. Capstone Project Advisor:

Signature: \_\_\_\_\_ Date \_\_\_\_\_

Print Name/Department: **Clark T.-C. Nguyen / EECS**

2. Faculty Committee Member #2:

Signature: \_\_\_\_\_ Date \_\_\_\_\_

Print Name/Department: **David J. Allstot / EECS**

**Transistor Circuits for MEMS Based Transceiver**

by

Kelvin Liang

A project report submitted in partial satisfaction of the  
requirements for the degree of  
Master of Engineering

in

Electrical Engineering and Computer Science

in the

GRADUATE DIVISION  
of the  
UNIVERSITY OF CALIFORNIA, BERKELEY

Committee in charge:  
Professor Clark T.-C. Nguyen  
Professor David J. Allstot

Spring 2015

## **Transistor Circuits for MEMS Based Transceiver**

Copyright © 2015, by the author.  
All rights reserved.

Permission to make digital or hard copies of all or part of this work for personal or classroom use is granted without fee provided that copies are not made or distributed for profit or commercial advantage and that copies bear this notice and the full citation on the first page. To copy otherwise, to republish, to post on servers or to redistribute to lists, requires prior specific permission.

## ABSTRACT

In recent years, the push for low power wireless sensor networks has called for the introduction of RF-MEMS transceiver devices capable of operating on small batteries or small scales of scavenged power from sources such as solar and kinetic energy. The design of ultra-low power MEMS based transceivers stands to revolutionize the fields of industrial monitoring, environmental monitoring, and biomedical imaging [1].

This report demonstrates a MEMS based transceiver capable of supporting these low power applications, and presents an industry/market analysis of a potential application. This report includes the design and simulation results of the transistor circuits, designed in 180nm TSMC, used in the MEMS based transceiver. The entire system is estimated to consume 115uW of power at a  $V_{DD}=1.8V$ . The transceiver system implements an FSK modulation scheme and takes advantage of a MEMS resonator, an oscillator, an envelope detector, a comparator, a power amplifier, and an output buffer. Individually, the oscillator consumes 15uW of power, the envelope detector consumes 410nW of power, the comparator consumes 237nW of power, and the power amplifier consumes 100uW. The system is currently optimized for data rates of 5kbps, but can easily support much higher data rates. This design currently operates at 60MHz VHF, but the tunable nature of the MEMS device allows for use of frequencies up to UHF [1].

## TABLE OF CONTENTS

PROBLEM STATEMENT .....	7
INDUSTRY, MARKET, AND TRENDS .....	8
Need For MEMS Based Transceivers.....	8
Competitive Landscape.....	9
Potential Applications and Customers .....	13
TECHNICAL CONTRIBUTIONS.....	16
Project Overview.....	17
Literature Review.....	18
Methods and Materials.....	25
Technical Contributions .....	31
SYSTEM SUMMARY .....	35
Oscillator.....	35
Envelope Detector.....	39
Comparator.....	46
Complete Receiver Chain .....	48
Power Amplifier.....	49
Transmit Chain.....	53
Voltage Buffer.....	54
CONCLUSION.....	60
WORKS CITED .....	61

## LIST OF FIGURES

Figure 1. Radio Front Ends a) Analog Receiver b) Digital Receiver c) Transmitter [17] .....	19
Figure 2. FCC Spectrum from 10 to 30 MHz [18].....	21
Figure 3. Channel Selecting and Interference [19] .....	21
Figure 4. AM Detector [20] .....	22
Figure 5. MEMS Transceiver [19].....	23
Figure 6. OTA Based Envelope Detector [26].....	27
Figure 7. Differential Envelope Detector [28] .....	28
Figure 8. BJT Envelope Detector [27] .....	28
Figure 9. Single Ended Source Follower Envelope Detector .....	29
Figure 10. Temperature Independent Current Reference .....	30
Figure 11. Envelope Detector and Current Reference .....	31
Figure 12. Noise Equivalent Circuit .....	32
Figure 13. Noise Plot .....	32
Figure 14. Minimum Detectable Signal .....	33
Figure 15. Layout of Oscillator and Envelope Detector .....	34
Figure 16: Pierce Oscillator .....	36
Figure 17: Growing Waveform Of The Oscillator.....	37
Figure 18: Power Consumption Of The Oscillator .....	37
Figure 19. Stimulating Circuit .....	38
Figure 20. Output Waveform of Oscillator .....	38
Figure 21. MEMS Resonator Model .....	39
Figure 22. Single Ended Source Follower Envelope Detector .....	41
Figure 23. Noise Equivalent Circuit .....	41
Figure 24. Noise Plot .....	42
Figure 25. Minimum Detectable Signal .....	42
Figure 26. Temperature Independent Current Reference .....	43
Figure 27. Envelope Detector and Current Reference .....	44
Figure 28. Layout of Oscillator, Current Supply, and Envelope Detector.....	44
Figure 29. Comparator Schematic .....	46
Figure 30. Comparator Functionality .....	47
Figure 31. Receiver Chain .....	48
Figure 32. Verification of Receiver .....	49
Figure 33. Class D & E Amplifier models [34] .....	50
Figure 34. Architecture of the Power Amplifier .....	51
Figure 35. Power Amplifier Schematic.....	51
Figure 36. Power Amplifier Layout.....	52
Figure 37. Measured Power Gain & Efficiency.....	52
Figure 38. Transmit Waveform.....	53
Figure 39. Temperature Independent Current Reference .....	56
Figure 40. Transistor-level Topology For Wideband Op-Amp .....	56
Figure 41. Wideband Op Amp Connected In Unity-gain Feedback.....	57
Figure 42. Transistor-level Topology Of The Rail-To-Rail Op Amp.....	58
Figure 43. Rail-To-Rail Op Amp Connected In Unity-gain Feedback .....	59



## PROBLEM STATEMENT

The capstone project highlighted in this report proposes a low power wireless transceiver that operates on 115uW of power. This is possible because of an integrated low power circuit using a Micro-Electromechanical System (MEMS) that acts as the resonator for the transceiver system. This is a significant feature because typical transceivers use quartz resonators instead of MEMS resonators and low power designs were not achievable with traditional resonators. State of the art transceivers for standards such as low-power Wi-Fi consume milli-watts of power using conventional resonators, which is about 100 to 1000 times more power consumption than the wireless transceiver created in this project. Operating at only 115 microwatts, this transceiver can be equipped with a small coin battery and run for decades. Systems employing the MEMS based transceiver can also be powered with energy harvesting sources such as miniature solar panels typically found on calculators, or kinetic energy storage devices typically found in many wristwatches. Some of the applications include long lasting mobile devices, intelligent medical implants, long lasting medical hearing aids, and animal tracking devices. In the booming Internet of Things (IoT) industry where many set-and-forget sensors are used, low power transceivers are needed to enable efficient wireless communication and MEMS based transceivers can be the answer. The applications of this technology are endless and any device that needs a wireless connection can benefit from the MEMS transceiver. The goal of this capstone project was to design the schematic of a fully functional MEMS transceiver that operates on 115 microwatts of power. This device has been successfully achieved.

## INDUSTRY, MARKET, AND TRENDS

This chapter provides a detailed industry analysis of our technology by first identifying the need for MEMS based transceivers. This chapter then identifies other competing technologies already present in the market, potential applications, and possible customers. This chapter concludes by proposing a possible go-to-market strategy with our technology.

### Need For MEMS Based Transceivers

Before discussing about specific competing technologies to MEMS, it is important to appreciate the context of how transceivers operate and what are some design metrics for a good transceiver. This chapter will first distinguish the power advantages of our MEMS transceiver chip from other conventional transceivers. We will then show why these advantages are relevant by illustrating the need for minimizing power use in today's transceiver applications.

Transceivers allow for wireless communications by transmitting and receiving wireless signals. To avoid interference, signals traveling in the air must travel in different frequency channels. This often requires them to be converted into higher frequencies in a process called modulation. When the signal then reaches its destination, the receiver then needs to recover the original signal from the modulated signal in a process called demodulation. It is the job of the transceiver to modulate and demodulate signals being sent and received; it does this by using a resonator to generate a reference frequency that is tuned to the desired sending or receiving frequency.

When designing a transceiver chain, one of the most difficult problems is isolating the desired signal from other unwanted signals that are received from the antenna. Engineers define the Q

factor of a resonator as its ability to resonate at a specific frequency. Resonators with a low Q factor are less selective; they resonate not only at the tuned frequency, but also at other nearby frequencies.

For smaller channels, the Q of the resonator needs to be high in order to minimize insertion loss, or loss of signal strength [2]. Most conventional transceivers implement resonators that need additional filtering to isolate the signal.

Herein lies the advantage of MEMS technology. Electro-Mechanical resonators generate larger Q factors than conventional resonators. MEMS resonators provide record on-chip Q factors operating at gigahertz frequencies while still maintaining excellent thermal and aging stability [2]. In particular, the capacitive-gap RF MEMS resonator that we used for our MEMS transceiver circuit produces exceptionally high Q around 100,000 and can be tuned to select 1kHz-wide channels over a 80kHz range [1]. The high Q factors of MEMS resonators eliminates any steps involving additional filtering and takes away the power consumption overhead required for reducing insertion loss from the resonator. Eliminating the filtering step also results in a simpler design for the system as a whole. By implementing a MEMS resonator, we have achieved a transceiver design that operates on 115uW of power.

### Competitive Landscape

The biggest competitors to our MEMS-based wireless transceiver are chips designed for standards such as Wi-Fi, Zigbee, and Bluetooth. Therefore, we begin by proving our transceiver

technology as a viable competitor against these existing technologies due to a combination of comparable long distance capability, moderate data rates, and lower power consumption.

To show that MEMS based transceiver is a feasible technology, we now require a closer examination of the major competitors in wireless sensor applications. The most recognizable competing technology in wireless communications are chips supporting the WiFi standards. These chips are the biggest threat to our technology because of its wide use in applications from cell phones to computers. Because it is supported across many platforms, WiFi is even used extensively for smart wearable and connected medical device applications. Thus, WiFi takes a sizeable chunk of the sensing market that might need our technology. The cost per WiFi chip is moderately expensive at a bulk price of \$3 for 1000 chips [3]. Although this cost is on the high end, WiFi's biggest strength is that it is one of the fastest means of wireless communications in the industry. Supporting up to 11 to 54Mbps (megabits per second), WiFi takes a commanding lead over Bluetooth at 1Mbps [3]. This means that WiFi transfers data up to 54 times faster than Bluetooth. Our transceiver can be configured for high data rates but at the expense of additional power consumption. Therefore, to secure a special niche for low power and low cost, our design is not optimized for speed. We operate at speeds of 5kbps, which is much lower than WiFi. However, the relaxed speed constraint allows us to design our transceiver architecture to be much simpler than typical WiFi chips and less costly as a result of less transistors and area [4]. By using a simple design, our MEMS-based chip is expected to be less costly than alternative WiFi chips. Although WiFi is a major competitor in the wireless communications field, low power applications that do not require excessively high data rates should favor our transceiver over WiFi.

Zigbee is another wireless communication standard that is less recognizable because it does not directly target the consumer market. However, Zigbee is widely used in some battery powered systems such as home networks, and smart watches that require moderately long distance communications [5]. Zigbee accomplishes long distance travel with a mechanism known as mesh networking. Mesh networking is a method of having all the devices in a given area working together to transmit your information. For example, in city of 100 smart phones spread out evenly, information can be transmitted across the entire region by having phones send information to each other and successively passing data forward one phone at a time until the data reaches its the final destination. In the simplest sense, this type of networking is analogous to a relay run where runners pass the baton to subsequent runners until the finish line is reached. Generally, mesh networking techniques are more sophisticated than described above and offer additional features such as fault tolerance. By utilizing this method of communication, Zigbee is able to serve information across very long distances and therefore commands the market of long distance communications.

Our technology can also achieve long distance travel by using low frequency techniques. High frequency networks that do not use mesh techniques cannot travel far because higher frequency signals have a larger probability of disappearing when coming into contact with obstructions like buildings. In comparison, lower frequency signals can wrap around obstructions without losing data. Therefore, implementing low frequency signals in our design allows us to compete with Zigbee's long distance travel. A weakness of using Zigbee chips is that they require consistent power draw in order to accurately pass information through successive nodes. In networks of

battery powered cell phones, Zigbee will drain batteries rapidly. Our transceiver chip easily beats Zigbee in power consumption because our chip does not need to be powered on at all times to achieve long distance travel. The clear advantage that Zigbee has in addition to long range is that their data rates are higher at 500kbps. However, much like the argument against WiFi, our design relaxes the speed constraint for optimizing cost and power consumption. Our chip has the competitive advantage in markets that require low cost, low power chips for long-distance, battery-operated devices that can tolerate moderate data rates.

So far, we have discussed Zigbee and WiFi chips as two major competitors of our technology. These two standards currently dominate the long distance travel market and the wearables market, respectively. Our transceiver chip hopes to capture some market share by offering low power alternatives with comparable long distance capability for battery powered devices. However, it should be said that Zigbee and WiFi are not the only two competitors. The wireless communications industry is a saturated field and there are several other standards that carved out their own niches.

The final competing wireless technology discussed in this chapter is Bluetooth. Bluetooth is a global wireless technology standard that enables convenient, secure connectivity for an expanding range of devices and services. This is a widely used communication channel for sharing voice, data, music and other information wirelessly between paired devices such as cars, medical devices, computers, and even toothbrushes. Its wide use poses a threat to our MEMS technology. Bluetooth runs at a high frequency carrier of 2.5GHz but is suitable for sending information only up to a range of 100 meters. As we have discussed in the case of Zigbee, we

can configure our system to communicate information over long ranges by choosing to operate at lower frequencies. Furthermore, the cost of Bluetooth is about 2.7\$ for 1000 chip-sets and we expect to operate at a smaller cost due to our simpler design methodology for our transistor circuits.

In the area of low power, Bluetooth Low Energy (BTLE), a newer version of Bluetooth developed in 2011, also poses a risk for our technology. BTLE ranks number one in the market for lowest energy consumption. Known as Bluetooth smart, this wireless standard extends the use of Bluetooth wireless technology to devices that are powered by small coin cell batteries such watches and toys. BTLE transceivers can allow these devices to run for years on a small battery. Although BTLE is currently the industry leader in low power transceivers, this technology still operates at power levels in the milliwatt range [6]. Our MEMS transceiver is designed to operate within a hundred microwatts of power, which will provide a significant power improvement to Bluetooth Low Energy chips.

### Potential Applications

Next, this chapter provides examples of applications that might use our low-power MEMS-based transceiver to show its relevance in the market today. The main interests of our technology will come from wireless sensor node markets, where low power and simplicity are much more important than data transmission rate [1]. Since the wireless sensor market is wide and diverse, this chapter uses body area network (BAN) sensors and environmental sensor networks (ESNs) as case studies to illustrate the needs for simple, low-power transceivers.

BAN sensors are used to collect information directly from the person's body. Designers integrate BAN sensors into smart textiles to detect the wearer's heart rate, stress, motion, and energy expenditure [7]. A transceiver chip will then enable the sensors to send this physiological information to an interface where either the person or a medical professional can view it and form educated decisions. The biggest challenge with these devices is miniaturizing the BAN node and keeping it low power while maintaining a broad range of applications. A full on-chip application-specific implementation for BAN has already been designed using the wireless protocol Zigbee and consumes approximately 4mW of power when transmitting and receiving. A tiny lithium coin-cell battery can easily provide enough power for this radio. Although current implementations of BAN are functional, an approach to combine MEMS technology with ICs has already been discussed as the next step to further miniaturize the features of the BAN project [7]. If we decreased power consumption from the milliwatt range to the microwatt range using MEMS, the battery life will can increase by several orders of magnitude.

ESNs are another area where we can employ low-power transceivers. These sensors constantly monitor the natural environment to study how they work and detect natural hazards such as floods and earthquakes. The transceiver allows for communication between the sensors and a Sensor Network Server, where it can be viewed at a base station [8]. The biggest advantage of ESNs is that they allow us to monitor remote or dangerous areas that have long been inaccessible to study [8]. The designer of these sensors needs to satisfy both low power and low maintenance constraints; these will ensure that the system will operate with minimum intervention for sensor



maintenance or changing batteries. MEMS technology can provide the low power and simplicity needed for these sensor nodes.

So far, we have shown that some wireless sensor applications such as BANs and ESNs need ultra-low power transceivers. Since this project was recently completed, we currently have no actual end-users for our transceiver chip. In the next section of this report, we identify some potential stakeholders and customers that can benefit from this technology.

From the consumer's point of view, our low power chip means that consumers would no longer need to replace their battery often. The low power consumption of the transceiver also enables the use of energy harvesting techniques such as miniature solar panels to eliminate the need of batteries altogether. People using sensors implanted in the human body will find our technology very necessary. Implantable medical electrical devices are gradually becoming more feasible as an assisted medical treatment, especially for detecting biological signals that doctors can use to monitor the condition of the patient. These implantable devices need to be extremely low power to prevent any potential harm to the body. If the device consumes a low enough amount of power, the energy provided to the device can be acquired from the body itself through kinetic energy harvesting, allowing the device to operate for an indefinitely long period of time. For this reason, companies specialized in biomedical imaging may also be interested in our product.

Besides applications in the medical field, the market of our product can also be expanded to other broad fields. There is an immense need for smart connected sensors in the agricultural industry. In 2014, IBM composed a report which stated that 40% of food produced by developed

nations is thrown away. The IBM study also found that weather damages and destroys 90% of crops grown by farmers [13]. This statistic is disheartening considering the amount of people on this planet that can benefit from food. On top of that, farmers are dedicating precious natural resources such as water and land to grow the wasted food. Our transceiver technology can provide farmers with the wireless monitoring they need to improve crop yield and reduce food waste. Our transceiver technology will also offer a convenient and hassle-free solution for large farms where battery maintenance is a burden. Pursuing the sensor and wireless monitoring application can disrupt the agriculture industry, which is ready for technologies that can wirelessly gather soil and other weather information. Market researcher BCC expects the environmental sensing and wireless monitoring technology business to grow from \$13.2 billion in 2014 to \$17.6 billion in 2019 [14].

The analysis of the applications and consumer needs has shown several strong potential markets that require low power transceivers.

## TECHNICAL CONTRIBUTIONS

This chapter of the report will highlight the technical aspects of the report and how they were divided among the members of the capstone team. This chapter will identify my contribution to this project and provide information about the literature review conducted in the process of designing the envelope detector, the methods used in the design, and the simulation results.

### Project Overview

The Transistor Circuits for a MEMS Based Wireless Transceiver project was divided into four milestones: the schematic design of the transistor circuits, the schematic level simulation to verify circuit behavior, the layout of the transistor circuits to prepare the system for fabrication, and the post-layout verification to verify system behavior. The capstone group – Kelvin Liang, Darryl Yu, Soumya Mantha, Keli Hui, and Yuehan Xu – divided the milestones into tasks that could be achieved individually. These milestones first focused on the creation of the building blocks needed for the low power transceiver system. The blocks were divided with Kelvin working on the envelope detector, Han on the oscillator, Keli on the comparator, Soumya on the power amplifier, and Darry on the buffer circuit. After combining each individual building blocks, the remaining tasks called for preparation of the layout design.

The envelope detector that I designed is a key piece of the transceiver system because it serves to detect the information stored in wireless signals. Without the envelope detector, useful information cannot be extracted from the wireless signals in the air. In order to place the envelope detector circuit into a stable state of operation, I also designed a temperature

independent current source. Without a stable current source, the system will lack robustness because the state of operation of electronic circuits can vary unexpectedly with temperature. The current source was a crucial piece of circuitry because it was also utilized by several of the other building blocks such as the oscillator and buffer. This part of the report will highlight the envelope detector and current source as my major individual contributions to this capstone project. This part of the report will also discuss my layout design of the envelope detector, current supply, and oscillator.

## Literature Review

The MEMS transceiver design discussed in this report pertains to the field of radio frequency and analog circuit design, and it both builds upon and advances existing bodies of work. In order to properly demonstrate the merits of a MEMS based transceiver, I must first discuss the challenges facing existing transceiver technology found in many publications and technical reports.

A transceiver is a system capable of transmitting and receiving wireless information, and can be found in devices such as radios, cell phones, tablets, and computers. Typical transmitter and receiver designs, such as the one shown in Figure 1, employ the following building blocks: an antenna, a low noise amplifier (LNA), a power amplifier (PA), a mixer and local oscillator (LO) pair, a filter, and a demodulator. In receivers, the wireless signal is captured by the antenna and travels from the left blocks to the right blocks in Figure 1. For transmitters, similar building blocks are employed, but the signal will travel through the blocks in the opposite direction from right to left and exit the antenna to enter the air.

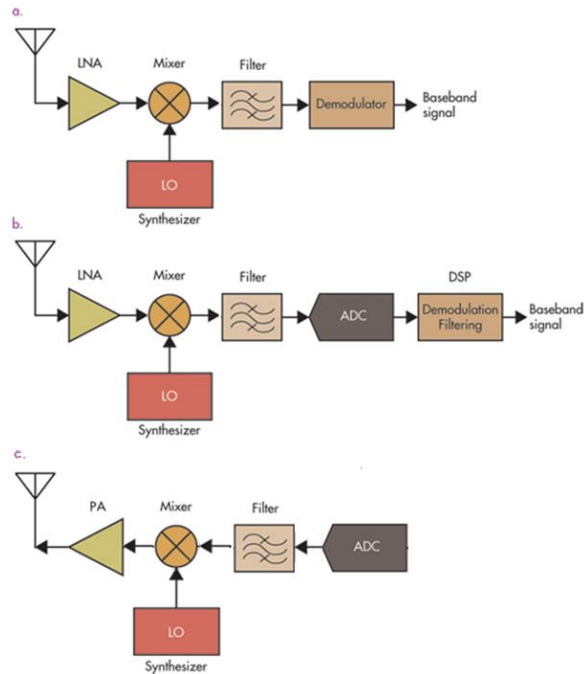


**Figure 1. Radio Front Ends a) Analog Receiver b) Digital Receiver c) Transmitter [17]**

Each block used in transceivers is an electronic circuit that serves a specific purpose:

- Antenna:

The antenna is non-discriminatory and captures all the wireless signals present in the air around the system. Because there are many different types of signals in the air around us, the transceiver needs to be able to differentiate the desired signal from undesired signals from sources such as cellular, internet, satellite, radio, and emergency communications.

- LNA:

Once the signal reaches the LNA stage, the data will be masked by electronic noise that is unavoidable and so the LNA serves to amplify the desired signal so that is not lost in the noise. In technical terms, the LNA serves to increase the signal-to-noise ratio or SNR.

The LNA is achieved through electronic circuits and requires careful design because it

can also introduce additional unwanted noise into the system. Circuit designers are often limited by the noise figure (NF) specification, which describes how much SNR degradation is caused by the stage. In addition, amplifier blocks such as the LNA typically provide gains at about 20dB (100 times amplification) and as such, consume a lot of power.

- Mixer and LO:

In receivers and transmitters, the desired signal is usually modulated into a carrier frequency to avoid congestion and interference. The Federal Communications Commission (FCC) has allocated different frequency spectrums for different applications and depending on the type of application, transmitters and receivers will have to operate at the allowed frequency. For example, AM radio is limited from 535kHz to 1605kHz frequency range. A snippet of the FCC spectrum, shown in [Figure 2](#), highlights the division of frequencies in the 10 to 30MHz range. The desired signal is modulated in transmitters with a mixer before leaving the antenna. The local oscillator provides the reference carrier frequency for the mixer to modulate the signal into the appropriate operating frequency. The signal can also be demodulated into a lower frequency, known as the intermediate frequency, in receivers with a mixer. The mixer is achieved through electronic circuitry and requires careful design because it can also add interference to the desired signal. Mixer designs are often limited by linearity specifications such as IIP3 and P1dB which describe how much interference is added by the stage. Conversion gain of a mixer is another specification that describes if the mixer introduces loss or gain for the system as it modulates and demodulates. State of the art standalone mixers are shown to consume several hundred microwatts of power [23].

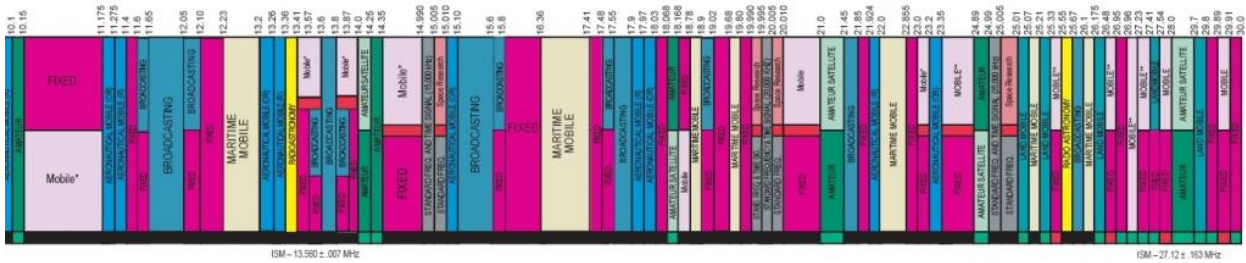


Figure 2. FCC Spectrum from 10 to 30 MHz [18]

- Filter:

This stage usually includes some channel tuning so that system can process the desired signal and reject the undesired signals. As shown in Figure 3, the tuning or channel select mechanism needs to adequately filter out signals at undesired frequencies or else the system will experience interference from adjacent channels. For example, analog radios employ tuners to capture different radio station channels and inadequate tuning can cause the radio to display sounds from multiple stations at once. The dotted line around the desired signals labeled TxA and TxB in Figure 3 indicates an ideal filtering mechanism. The greatest challenge facing filters is the ability to create filters with ideal characteristics because most filters are wider and will not completely reject the interferers.

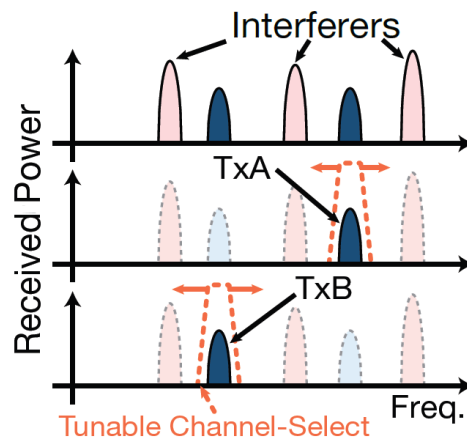
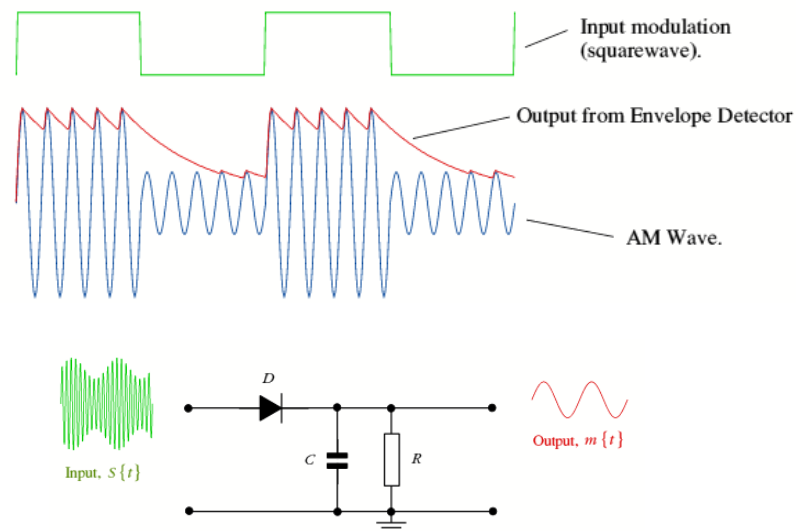


Figure 3. Channel Selecting and Interference [19]

- Demodulator:

Once the signal has reached this stage, it is processed with a demodulator to extract the useful information, and depending on the modulation scheme employed, different demodulators are used at this stage. For example, amplitude modulation (AM) stores the information in the amplitude of a signal and frequency modulation (FM) stores the information in the frequency. In the case of AM radio where the information is stored in the amplitude, a simple demodulator could be a device that measures the amplitude of the signal over time. In frequency domain, an AM detector can be achieved with a band pass or low pass filter that captures the peaks, or low frequency content, of the signal.



**Figure 4. AM Detector [20]**

Our MEMS based wireless transceiver allows us to differ from many of the existing and proposed technologies by eliminating the need for many of the power hungry building blocks used in traditional architectures. This reduction in the overhead power requirement, paired with the low power MEMS resonator device, has allowed for the creation of a system that consumes



115 microwatts of power. Systems like the one proposed in [21] are designed to consume 1.8mW of power, which is about 15 times less efficient than our system. Our capstone project is advancing the field of radio frequency circuit design by opening the door for low power applications, longer lasting devices, and more robust systems.

The schematic shown in Figure 5 demonstrates the system level concept of the MEMS based transceiver proposed by our mentors Professor Clark Nguyen, Dr. Tristan Rocheleau and Thura Lin Naing. The simplicity of the design allows us to eliminate the need for blocks such as the LNA, mixer, and filter. Our capstone project built upon the concept proposed by our advisors by adding several key blocks and by physically implementing the design. The blocks that this team designed include an oscillator, an envelope detector, a comparator, a buffer and a power amplifier.

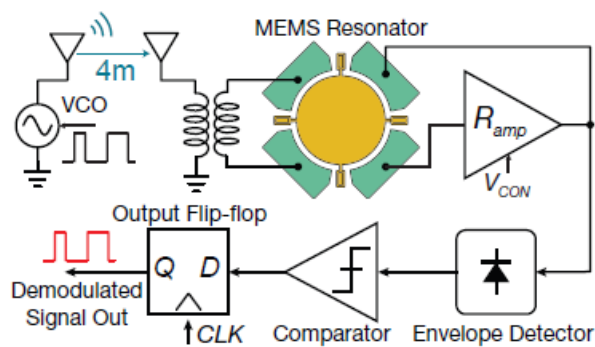


Figure 5. MEMS Transceiver [19]

The MEMS (microelectromechanical system) resonator, is the first stage of the transceiver. The remaining design of the transceiver required various electronic transistor circuits created in 180nm complimentary mosfet (CMOS) technology. The individual building blocks of the transceiver serve the following purposes:

- MEMS Resonator:

The MEMS resonator is a high Q factor device that allows for highly selective tuning and filtering. In this application, the Q factor describes the degree of selectivity and unlike the typical architectures and filters shown in Figure 1, the filtering from the MEMS device eliminates interfering signals with extremely high attenuation. In addition, the tunable nature of the MEMS resonator means we can select many different channels or frequencies and because of this, the system can be designed to support multiple standards.

- Oscillator:

The oscillator, much like the local oscillator seen in traditional architectures, serves as a reference carrier signal. The oscillator is designed to feedback the signal to the MEMS device to generate sustainable oscillations. Because the system employs frequency shift keying (FSK) as the modulation scheme, the information is stored in the frequency of the signal that is generated by the oscillator. In the case of this design, the oscillator operates at 60MHz and the resonator converts the frequency information into amplitude information via growing oscillation amplitudes.

- Envelope Detector:

The output of the oscillator is fed into an envelope detector to extract the information stored in the growing oscillations. Similar to [Figure 4](#), the envelope detector measures of the peaks of the oscillations to extract the stored binary information.

- Comparator:

The binary information (1 or 0) is then decoded from the envelope detector's peak amplitude information by using a comparator and a threshold level. If the amplitude from

the output of the envelope detector is above the threshold, the data is triggered to be a 1, and if the amplitude is below the threshold, the data is triggered to be a 0. With this comparing mechanism, our transceiver can successfully recover the desired waveform consisting of 1's and 0's.

- Buffer:

A buffer circuit is added to the system to allow for probing and debugging after the fabrication process.

- Power Amplifier:

In transmitting data, a power amplifier is needed to convert the input signal into a significant amount of radio power that is suitable for transmission of the wireless signal[24].

The envelope detector that I designed built upon existing bodies of work. In the methods and materials section of this report, I highlight many of the challenges facing existing envelope detector architectures that can be found in publications and technical reports.

## Methods and Materials

In designing the envelope detector for the system shown in Figure 5, I kept in mind the intended application of the transceiver. First and foremost, the envelope detector needed to be extremely low power because the entire system had to consume about 115 microwatts of power and the majority of the power budget was allocated for the power amplifier and oscillator. Therefore, the final design of my envelope detector needed to operate on nanowatts of power. Second, the envelope detector needed to be able to measure amplitude variations as small as several

microvolts. Third, the detector needed to be able to demodulate very low amplitude signals that are close to the noise floor. Fourth, the envelope detector could not introduce too much additional noise into the system. Lastly, the envelope detector needed to be temperature independent because any variation to the bias level of the circuit will affect the threshold level of Keli's comparator. All of these specifications turned what would've been a simple design into a complicated circuit. The method and approach I took in accomplishing my goal of designing a circuit meeting the above specifications included a thorough review of known circuit topologies.

Classic envelope detectors are simple to design because they require a basic diode and low pass filter circuit. However, to meet the specifications laid out above, the envelope detector I designed needed to be based off an entirely different architecture. The main issue with using the classic diode detector with low pass filter circuit configuration is highlighted in a technical report published by Professor Jan Rabaey and Postdoc Researcher Simone Gambini of UC Berkeley [25]. According to the report, a significant amount of gain needs to be applied to the radio frequency signal prior to entering the envelope detector because the signal can pass through the detector only if the amplitude is above the diode semiconductor turn-on voltage. In other words, if the amplitude is not high enough, the signal will not pass through the detector and will not be demodulated properly. In our low power application, the amplitude of the input signal is estimated to be in the millivolt range which is far below the required minimum .7V turn-on voltage of nominal discrete diodes. A solution to this problem would be to apply the necessary gain to the signal prior to the envelope detector, but this would mean higher power consumption. In an effort to find a suitable low power solution to resolve this problem, I attempted topologies found in various publications. In an Institute of Electrical and Electronic Engineers (IEEE) publication by researchers from Seoul National University, an operational transconductance

amplifier (OTA) based envelope detector that consumes 6.3 milliwatts (mW) is capable of receiving signals of 257 millivolts (mV) [26]. However, the OTA based design shown in [Figure 6](#) consumes 54 times more power than the target power of the envelope detector needed for our system.

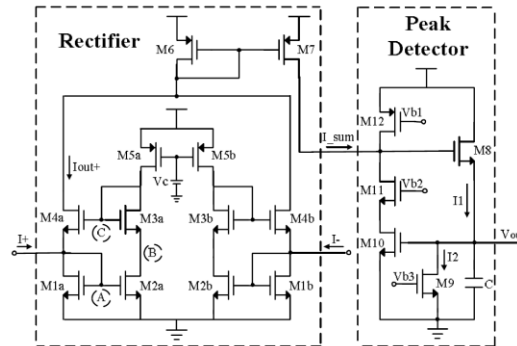


**Figure 6. OTA Based Envelope Detector [26]**

In another IEEE publication by Dr. Denis Daly from the Massachusetts Institute of Technology, a differential envelope detector capable of receiving signal amplitudes as low as 5mV is proposed [28]. However, Dr. Daly's envelope detector architecture ([Figure 7](#)) consumed far too much power at 10 $\mu$ W. In another paper by Professor Rabaey from UC Berkeley, a 1 microwatt envelope detector is proposed [29]. Unfortunately, the 1 $\mu$ W power consumption was also too much for our application and could not be reduced further.

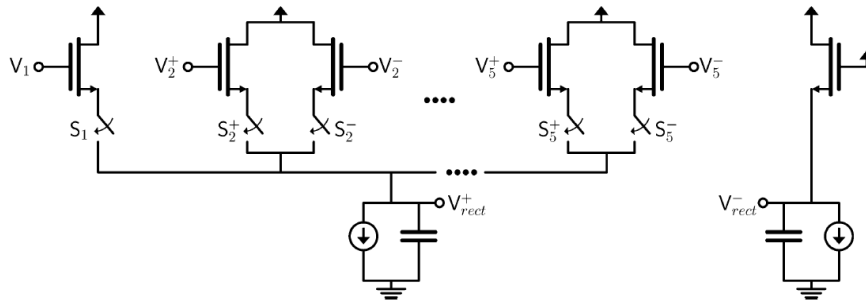


**Figure 7. Differential Envelope Detector [28]**

Finally, I settled for a source follower circuit with a peak detection capacitor at the output. The motivation for this design came from a publication by Professor Robert Meyer from UC Berkeley [27]. The design proposed by Robert Meyer, shown in Figure 8, was based off of bipolar junction transistors and consumed 20-50 microwatts of power.

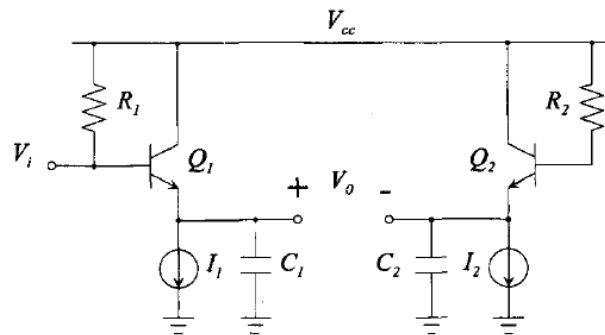


**Figure 8. BJT Envelope Detector [27]**

I built upon the design shown in Figure 8 by implementing the topology in 180nm CMOS transistors. I also converted the design into a single ended implementation, added a PMOS in triode for high frequency rejection, and successfully lowered the power consumption to 167.1 nanowatts (nW). I also added a copy of the input branch that is used to supply the bias voltage as a reference voltage for the comparator. The envelope detector I designed is shown in Figure 9 and is capable of recovering signals with amplitudes as low as 2mVpp, which is an improvement on the higher power designs proposed by researchers at other universities. Through simulations

in Cadence and the ADE tool suite, I was able to confirm the operation of the envelope detector. Those simulation results can be found in the next section of this report.

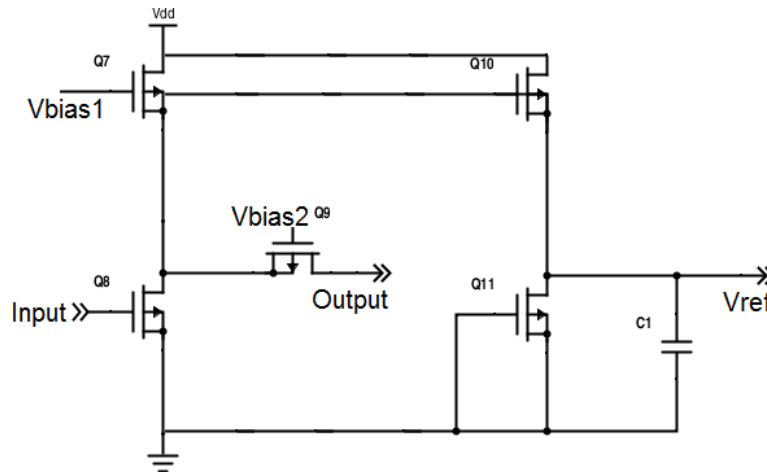


**Figure 9. Single Ended Source Follower Envelope Detector**

After successfully creating a low power envelope detector suitable for our transceiver system, the next daunting task was designing a current reference capable of supplying 83 nanoamps (nA) of current. Because the circuit operated at such low power, I needed to design a very stable current reference to supply the extremely low current needed to bias the envelope detector. I began my design by referring to a circuit proposed by Keith Sanborn from the University of Arizona [31]. In his paper, Dr. Sanborn proposed a folded cascade with temperature dependence cancellation bandgap reference design that supplies 20 microamps ( $\mu\text{A}$ ) of current. Following Dr. Sanborn's example, I designed my current reference using the same method of generating a stable and temperature independent circuit.

The final design of my current reference is shown in [Figure 10](#) and is capable of supplying 83nA of current with a negligible .3% variation across the  $0^{\circ}\text{C}$  to  $70^{\circ}\text{C}$  temperature range. This

stability was achieved by cancelling the temperature dependence of the resistor in the circuit with a diode connected NMOS transistor in parallel. The low current supply was achieved using maximum long channel devices in 180nm TSMC transistors. The main issue that rises when operating at low currents is noise and this problem is further exacerbated because the current source directly biases the envelope detector. Therefore, the noise produced by the current source will degrade the input signal due to the unity gain source follower topology of the envelope detector [30]. An extensive noise analysis was conducted by hand and verified with simulation on Cadence. The results indicate that the noise generated by this low current reference is -142.5dBm at the 60MHz operating frequency.

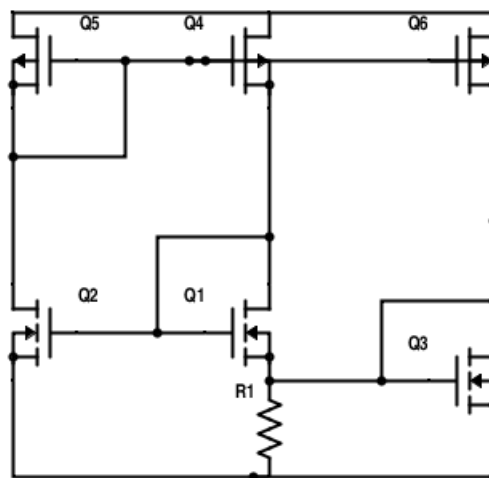


**Figure 10. Temperature Independent Current Reference**

With the design of the low power envelope detector and low current reference circuit complete, the building block is ready to be implemented into a working transceiver system. In the next sections, I will highlight the performance of the standalone envelope detector with current reference. I will also discuss the results of the system level integration with Han's oscillator and Keli's comparator to form the front end receiver.



## Technical Contributions

The final design of the envelope detector with current reference is shown in [Figure 11](#).

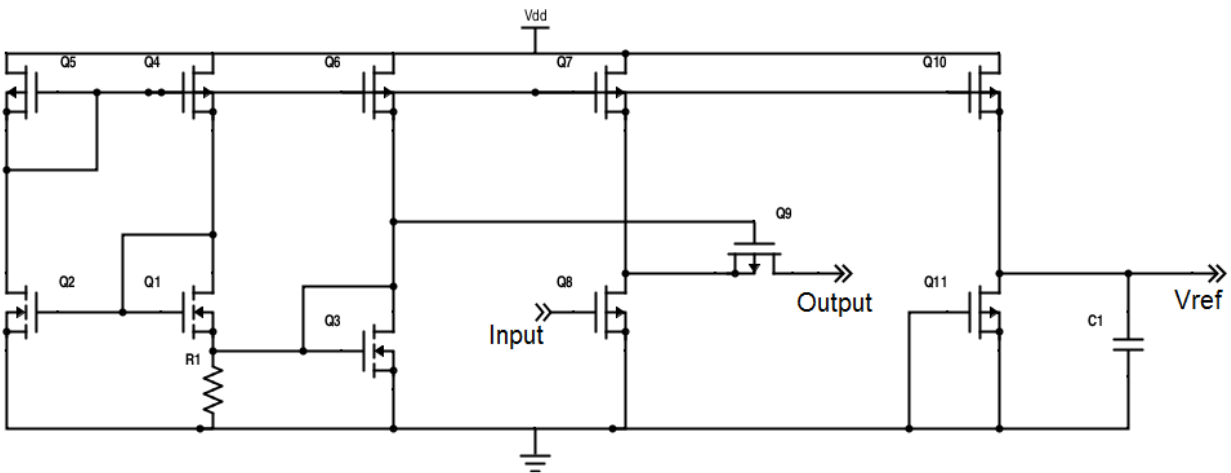


**Figure 11. Envelope Detector and Current Reference**

From the noise simulation discussed previously, the noise floor of the overall block is found to be -142.5dBm at the 60MHz operating frequency. The noise equivalent circuit used for the hand calculations is shown in [Figure 12](#). The noise simulation plots verifying the hand calculation is shown in [Figure 13](#). From the equation below, the minimum detectable signal with a nominal noise figure (NF) and signal-to-noise ratio (SNR) requirement is

$$\text{Min Det. Signal} = \text{Noise Floor} + 10\log(BW) + NF + SNR$$

$$\text{Min Det. Signal} = -53.9\text{dBm}$$

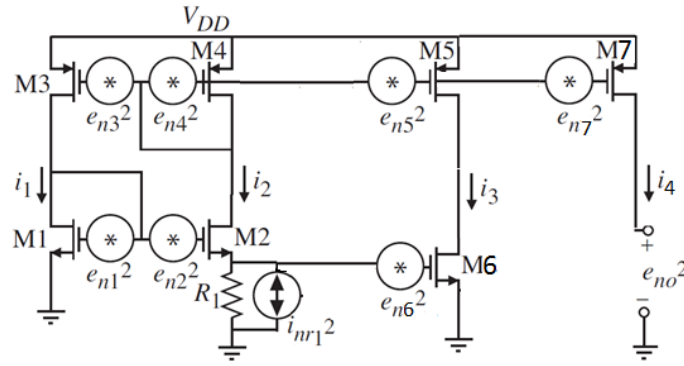


Figure 12. Noise Equivalent Circuit

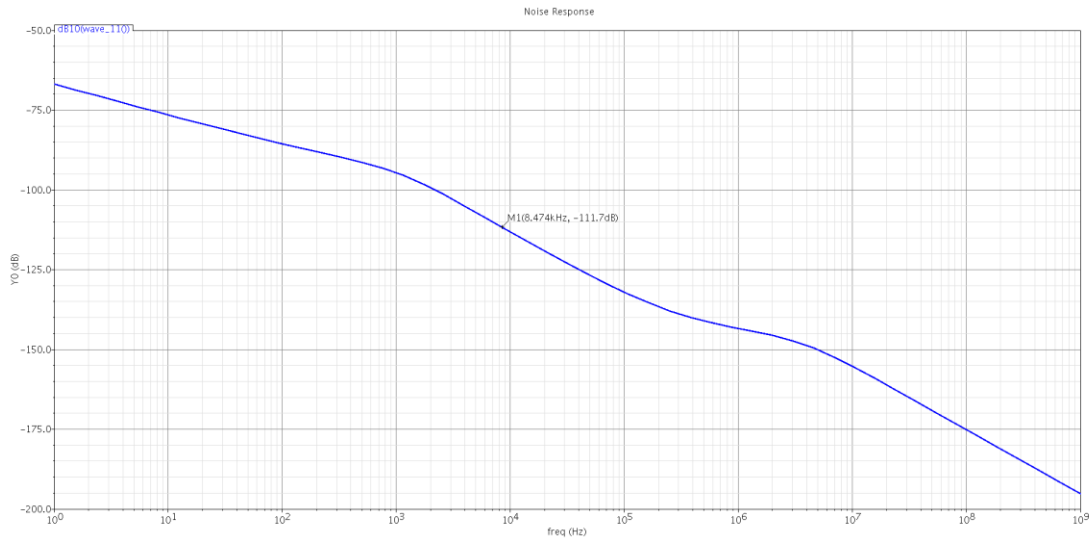
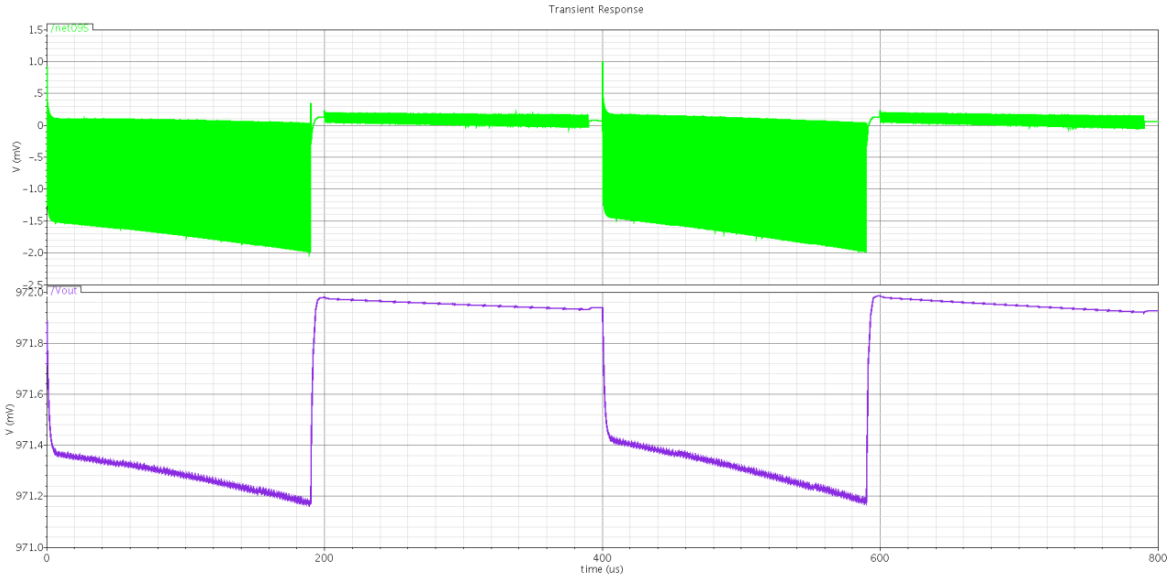


Figure 13. Noise Plot

Therefore, this envelope detector is capable of demodulating radio frequency signals with amplitudes as low as 2mVpp before the signal is overrun with noise. The simulation proving the ability to demodulate signals with 2mVpp amplitude is shown in Figure 14. On the other end of the spectrum, the maximum amplitude the envelope detector can detect before clipping is simulated to be 1V. Therefore, the dynamic range of this block is

$$0dBm - (-53.9dBm) = 53.9dB.$$



**Figure 14. Minimum Detectable Signal**

To reiterate, my goal for this particular building block was to design a low power envelope detector capable of receiving low voltage radio signals. Additionally, the low power envelope detector was to be biased with a stable low current reference. As shown in the simulation results, I was successfully able to accomplish these goals and my final design operates on 83nA on a 1.8V supply for a total consumption of 250.6nW. The current reference has four branches and with each branch drawing 83nA on a 1.8V supply, the total power consumption is 417.7nW. As hoped, the current reference is temperature stable with a negligible .3% variation over the 0°C to 70°C temperature range, and the envelope detector is capable of receiving signals at amplitudes as low as 2mVpp.

After successfully designing the crucial envelope detector block, the capstone team set forth with integrating all the blocks into a functional transceiver system. The results of that integration will be discussed in the final summary. We encountered many problems when implementing the entire system because we could not simply piece the individual building blocks together. We

discovered that some slight modifications needed to be performed before the system functioned properly.

As part of the integration process, I also designed the layout of the envelope detector schematic and the oscillator. The results of the layout is shown in [Figure 15](#) and final area for this layout is  $750\mu\text{m}^2$ .

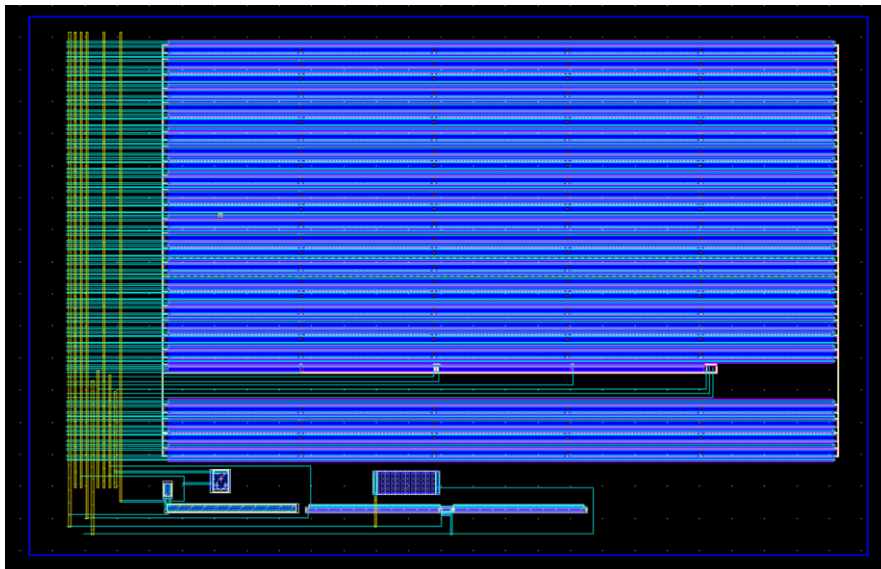


**Figure 15. Layout of Oscillator and Envelope Detector**

## SYSTEM SUMMARY

This chapter of the report will provide the summary of the system level integration and performance of the receiver and transmitter. This chapter will provide a summary of the oscillator, comparator, power amplifier, and buffer blocks. For cohesiveness, this chapter will also include an abridged version of my technical contributions in the envelope detector.

### Oscillator

The function of oscillator in a transceiver system is to create a constant high frequency signal to carry the information signal. In a transmitter system, the oscillator output modulates the information signal, and the power amplifier amplifies the signal to be transmitted afterwards. In the receiver chain, the oscillator and envelope detector demodulates the transmitted signal and then sends it to comparator for decoding.

The oscillator in this system is designed as a MEMS-Based oscillator, where the MEMS device is used as a resonator to replace the crystal that is used in traditional oscillators. The advantage of the MEMS-Based oscillator is that it provides high Q to have a more accurate channel selection, and the simple design also contributes to low power consumption.

Oscillators typically consume the majority of power in the receive chain. Therefore, the topology of the oscillator determines the power consumption of whole system at some degree. Based on the low power consumption specification, the Pierce oscillator schematic, which consumes relatively low power, is being used. The schematic is shown below in [Figure 16](#):

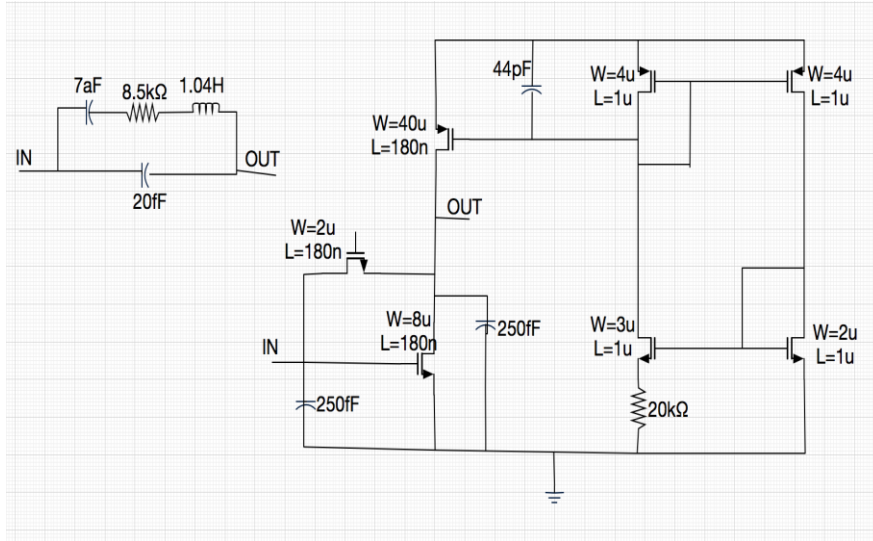


**Figure 16: Pierce Oscillator**

The feedback loop of this oscillator has a phase shift of  $360^\circ$ , and in order to make it oscillate, we also need to design for a negative resistance greater than  $8.5\text{k}\Omega$  looking into two ports of resonator. Since positive resistance consumes power, we can regard negative resistance as an energy source. If this “energy source” provides energy larger than the power consumption of resistor in the resonator, then this oscillator can work well.

According to the equation of negative resistance:

$$\text{Re}(Z_c) = - \frac{g_m C_1 C_2}{(g_m C_3)^2 + \omega^2 (C_1 C_2 + C_2 C_3 + C_3 C_1)^2}$$

In the circuit shown in [Figure 16](#), the nodes “IN” and “OUT” link with the MEMS device by bond pad connection, and we assume the parasitic capacitance on the bond pad is around  $250\text{fF}$ . The transconductance of the common source amplifier is  $165.68\mu\text{A/V}$ , and the value of negative resistance is  $13.66\text{k}\Omega$ .

The output waveform and power consumption is shown below in [Figure 17](#) and [Figure 18](#).

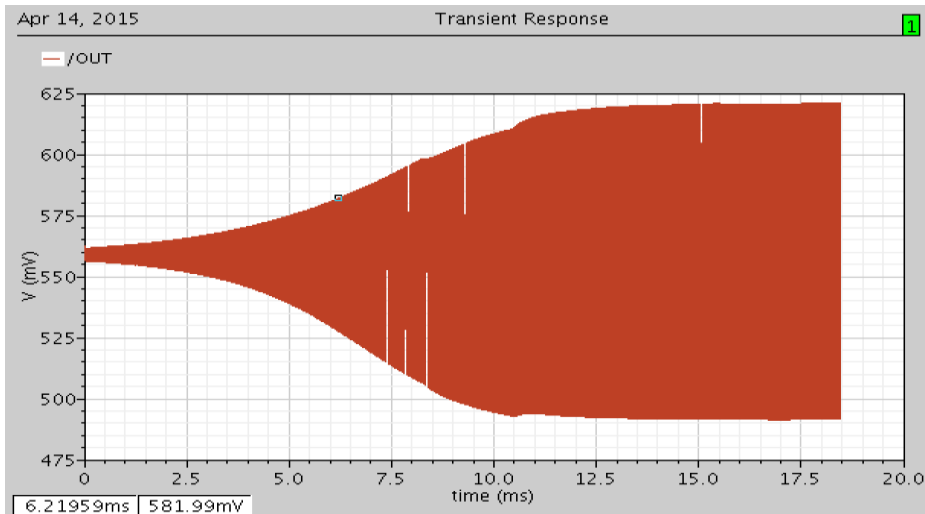


Figure 17: Growing Waveform Of The Oscillator

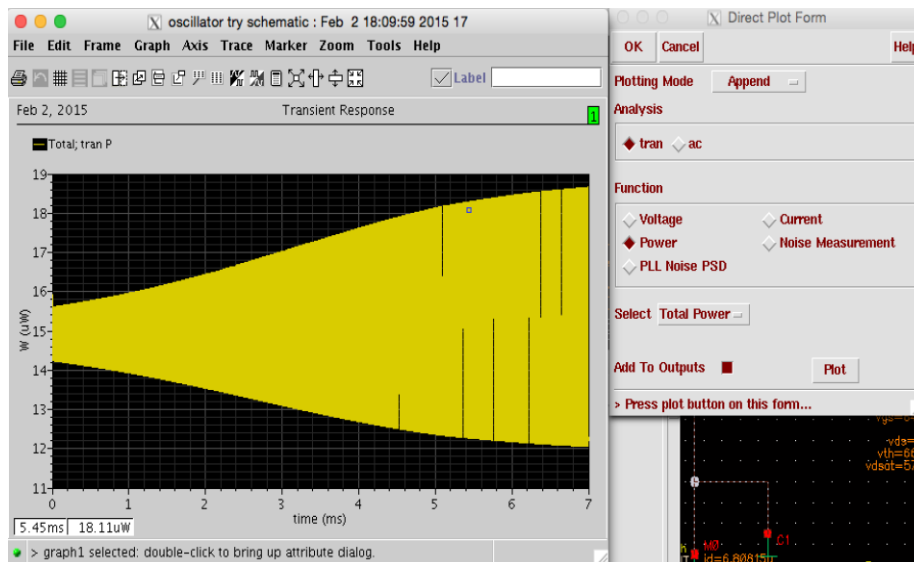


Figure 18: Power Consumption Of The Oscillator

The resonance frequency of 58.98MHz, and the amplitude is 128mV. The power consumption is 15uW.

The amplitude of the oscillator output in each period differentiates '1' and '0'. The simulation required different stimulating signals to generate the different growing speed. Further, the

oscillator required a reset to toggle a '0' in simulation. The reset to the oscillator was generated by switching the resonator resistance to a much higher resistance to destroy the quality factor.

The stimulating circuit with a reset is shown in [Figure 19](#).

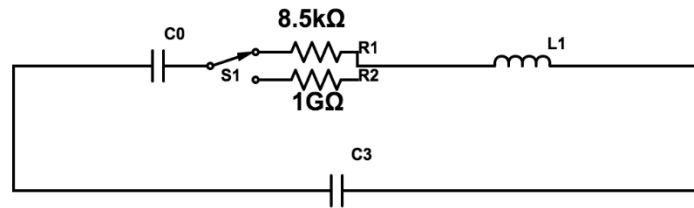


**Figure 19. Stimulating Circuit**

R1 corresponds to the working state, and R2 corresponds to resetting state. When the circuit switches to R2, the high resistance destroys the quality factor so that the oscillator can no longer work. The switch S1 is set to be periodically switches between R1 and R2. The output waveform is shown below in [Figure 20](#).

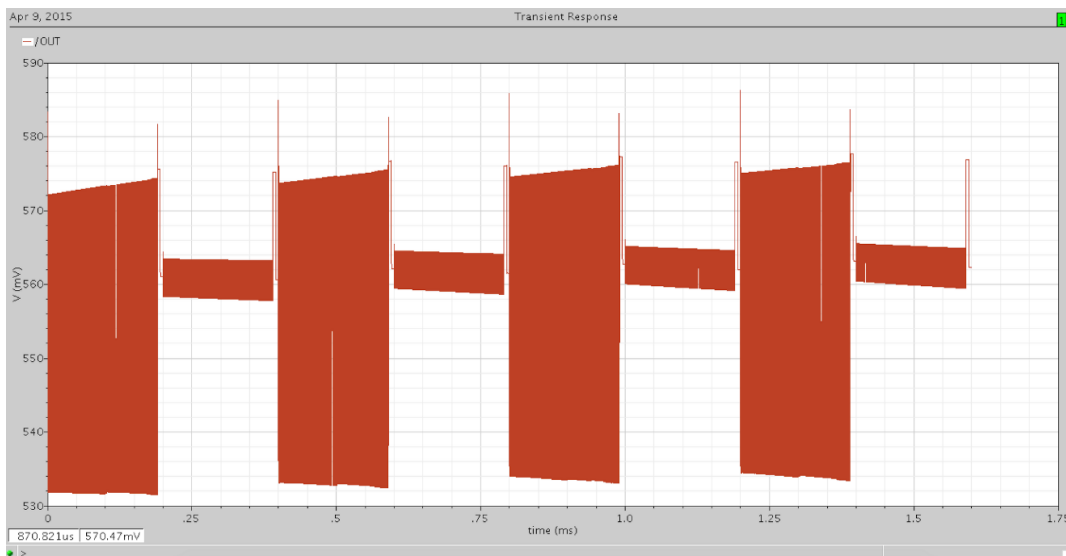


**Figure 20. Output Waveform of Oscillator**

In addition, an FSK signal is needed on the transmitter side. The method to generate an FSK signal is to switch the value of capacitance between two values.  $7\text{aF}$  capacitance was used to



generate 59MHz signal, and 6.5aF capacitance to generate 61MHz signal. The MEMS resonator model is shown below in [Figure 21](#):

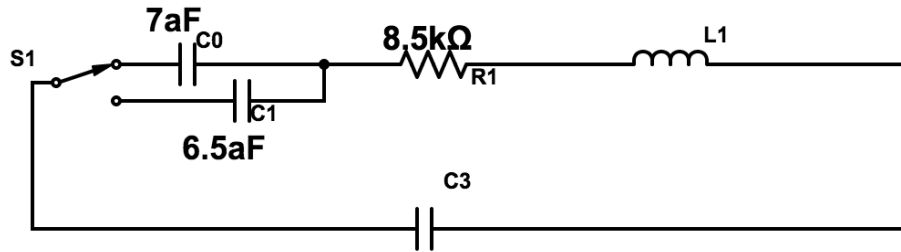


**Figure 21. MEMS Resonator Model**

Design Specification	Value
Resonance frequency	58.9MHz
Power Consumption	15uW

### Envelope Detector

The envelope detector designed is a key piece of the transceiver system because it serves to detect the information stored in the envelope of wireless signals. In order to bias the envelope detector circuit into a temperature stable state of operation, a temperature independent current source was implemented. This temperature independent current source was also taken advantage of by the oscillator and the buffer circuits.

The design of the envelope detector had several key specifications. The consumption of the envelope detector was limited to several nW. Second, the envelope detector needed to be able to measure amplitude variations as small as several microvolts with good carrier rejection. Lastly, the envelope detector needed to be temperature independent because any variation to the bias level of the circuit will affect the threshold level of Keli's comparator.

Classic envelope detectors are simple to design because they require a basic diode and low pass filter circuit. However, to meet the specifications laid out above, the envelope detector used in this system needed to be based off an entirely different architecture. The main issue with using the classic diode detector with low pass filter circuit configuration, as highlighted in [25], is the need for a significant amount of gain to bring the radio frequency amplitude above the turn on voltage of the diode. The high gain required in the classic diode detector is not suitable for our low power design. Many of the alternative envelope detector architectures capable of receiving low radio signals consumed far too much power. In [26], an operational transconductance amplifier (OTA) based envelope detector can demodulate signals as low as 257mV while consuming 6.3mW of power. In [27], [28] and [29], differential envelope detectors capable of receiving RF as low as 5mV consumed 20 $\mu$ W, 10 $\mu$ W and 1 $\mu$ W respectively.

The envelope detector implemented in this transceiver was designed with 180nm TSMC process. The design implemented a single ended source follower stage with low bandwidth to filter out the carrier. A PMOS biased in the triode region is used in the output stage for capacitive low pass filtering. A copy of the input branch is also used to supply the DC bias voltage as a reference voltage for the comparator. The final envelope detector, shown in [Figure 22](#), is capable of recovering signals with amplitudes as low as 2mVpp. Overall, the envelope detector consumed 167.1nW of power.

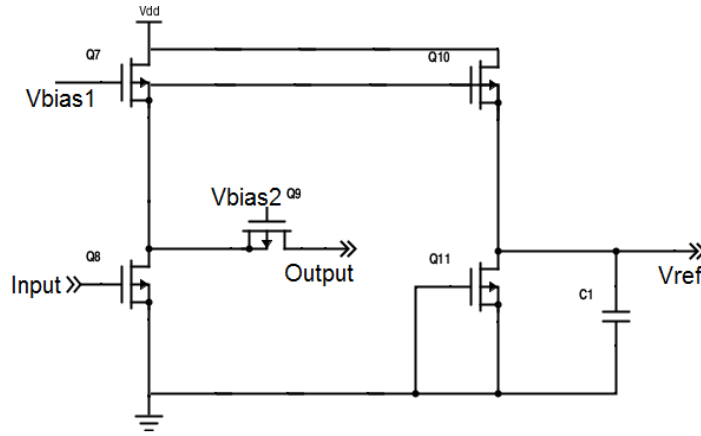


**Figure 22. Single Ended Source Follower Envelope Detector**

The noise equivalent circuit used for the hand calculations is shown in [Figure 23](#). The noise simulation plots verifying the hand calculation is shown in [Figure 24](#). From the equation below, the minimum detectable signal with a nominal noise figure (NF) and signal-to-noise ratio (SNR) requirement is

$$\text{Min Det. Signal} = \text{Noise Floor} + 10\log(\text{BW}) + \text{NF} + \text{SNR}$$

$$\text{Min Det. Signal} = -53.9\text{dBm}$$

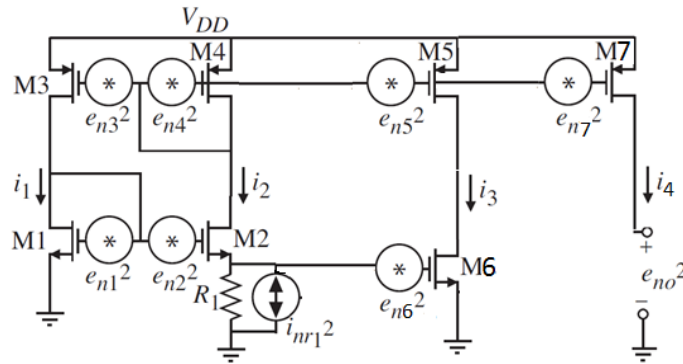


**Figure 23. Noise Equivalent Circuit**

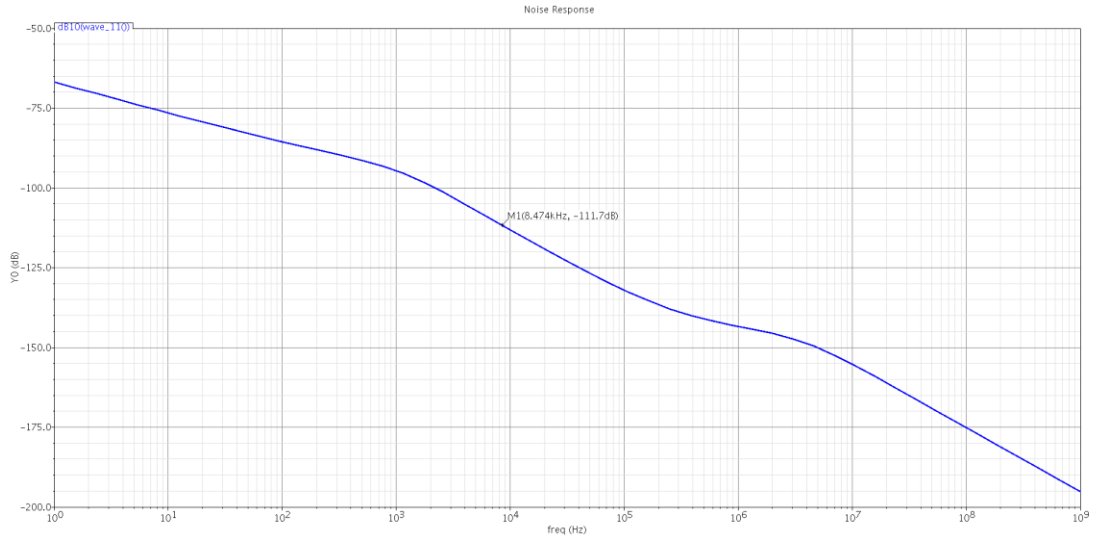


Figure 24. Noise Plot

Therefore, the minimum detectable is 2mVpp. The simulation proving the ability to demodulate signals with 2mVpp amplitude is shown in Figure 25. On the other end of the spectrum, the maximum amplitude the envelope detector can detect before clipping is simulated to be 1V.

Therefore, the dynamic range of this block is

$$0dBm - (-53.9dBm) = 53.9dB.$$

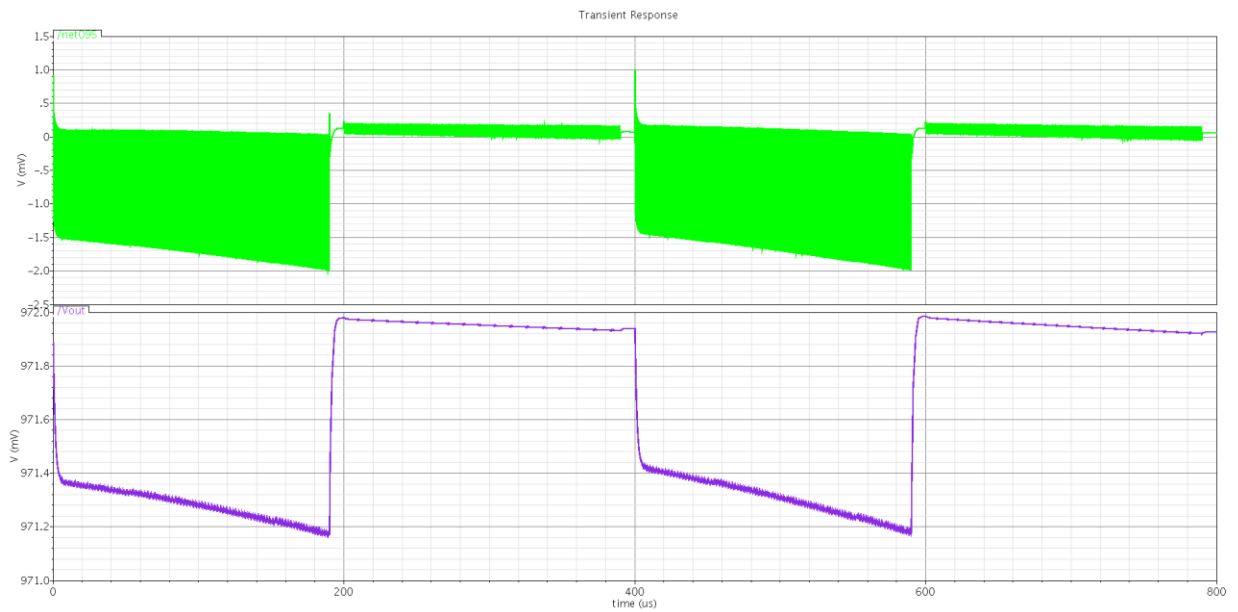


Figure 25. Minimum Detectable Signal

The envelope detector discussed was biased with 83nA of current and required stable reference supply. The design of the reference followed the methodology proposed in [30], which discusses a stable bandgap reference. The final design of the current reference is shown in Figure 26 and is capable of supplying 83nA of current with a 0.3% variation across the 0°C to 70°C temperature range. This stability was achieved by cancelling the temperature dependence of the resistor in the circuit with a diode connected NMOS transistor in parallel. The low current supply was achieved using maximum long channel devices in 180nm TSMC transistors.

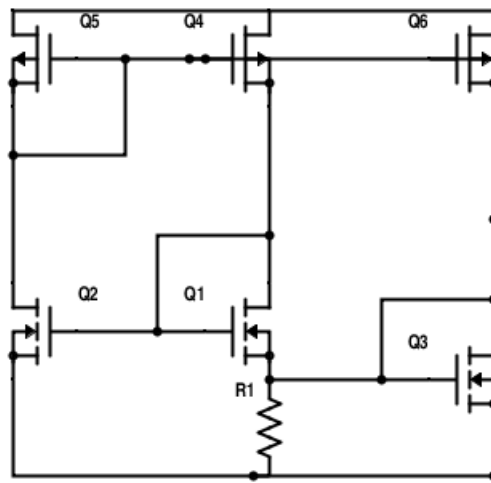
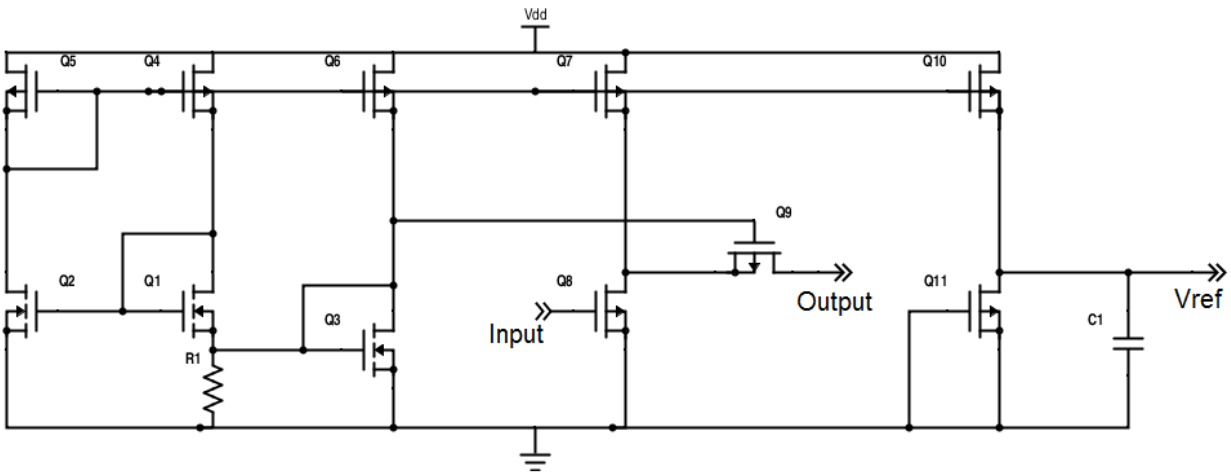


Figure 26. Temperature Independent Current Reference

The final design of the envelope detector with current reference is shown in [Figure 27](#).



**Figure 27. Envelope Detector and Current Reference**

As part of the integration process, the layout of the envelope detector, current reference and the oscillator was designed. The layout is shown in [Figure 28](#) with a die area of  $750\mu\text{m}^2$ .

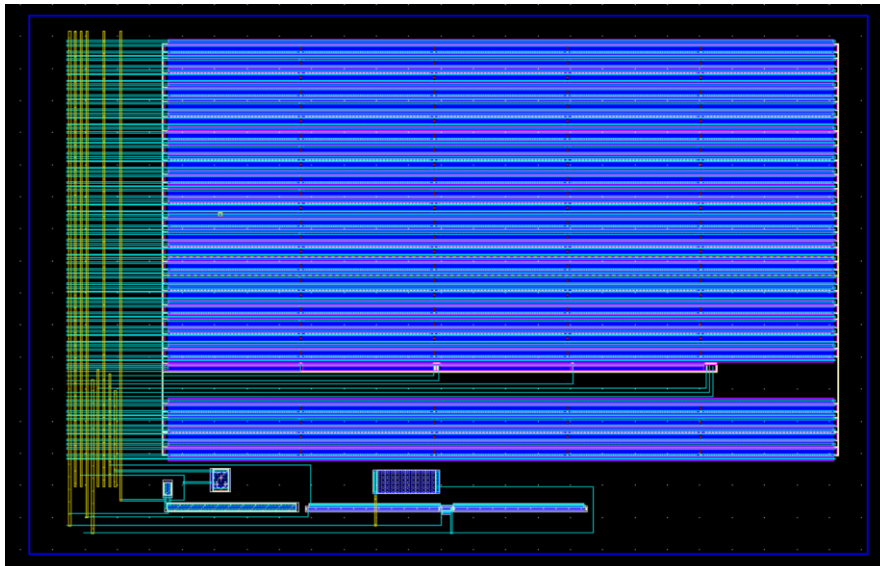


**Figure 28. Layout of Oscillator, Current Supply, and Envelope Detector**

<b>Block Summary</b>	
<b>Envelope Detector</b>	
Minimum Detectable Signal	2mVpp
Dynamic Range	53.9dB
Envelope Delay	.5us
Envelope Bandwidth	1MHz
Carrier Bandwidth	500MHz
Total Power Consumption	167.1nW
<b>Current Reference</b>	
DC Current 0°C	83.21nA
DC Current 25°C	83.55nA
DC Current 70°C	83.89nA
Total Power Consumption	250.6nW
<b>Layout</b>	
Die Size (Oscillator, Envelope Detector, Current Source)	750um <sup>2</sup>

## Comparator

When Frequency Shift Keying (FSK) modulated signals enter the transceiver, they give rise to the periodically restarted oscillations [1]. When the oscillation envelope is detected, the comparator should be able to discriminate “0”s and “1”s [1].

The schematic for the comparator is shown below in Figure 29.

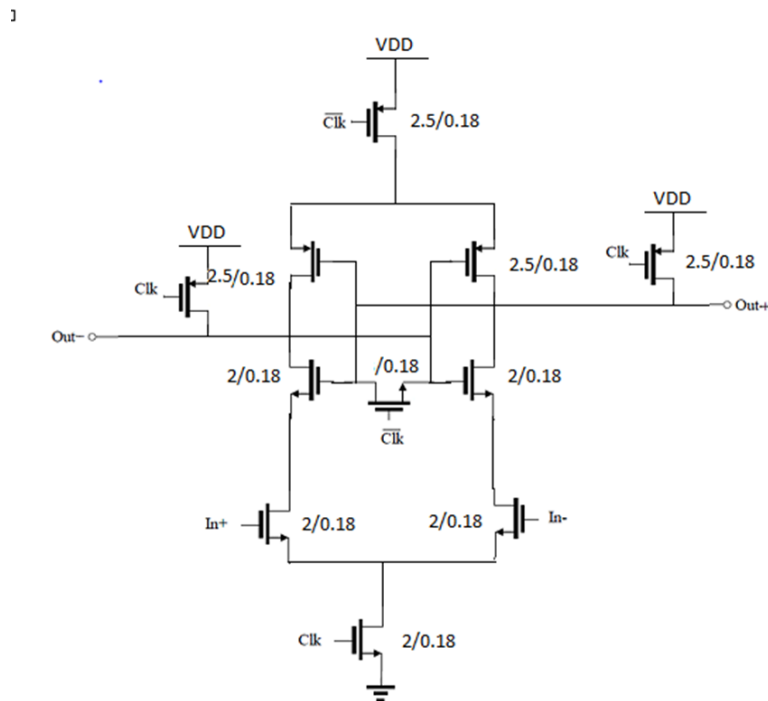


Figure 29. Comparator Schematic

The benefit of this design is that in the reset phase, when the clock signal is low, voltage supply and ground are disconnected from the latch. Therefore, no power consumption occurs in this phase. Since digital circuits normally only accept supply voltage and ground voltage as “1”s and “0”s, a PMOS pair was added to pull the output to supply voltage. During the evaluation phase,



when the clock signal is high, the comparator is powered and starts to compare the input signals at the “In+” and “In-” terminals. The latch circuit grows the input difference and finally reflects either “1” or “0” at the output terminal.

The functionality of the comparator is confirmed with Figure 30. The first plot is the input signal, the second one is the clock signal and the third one is the output signal. The test signal was a sinusoidal wave with 1mV amplitude at 800mV DC level. The reference voltage used to discriminate the “0” and “1” was 800mV. From the output signal plot, it is shown that when the clock is on, if the input signal is above 800mV, the output is “1”; vice versa.

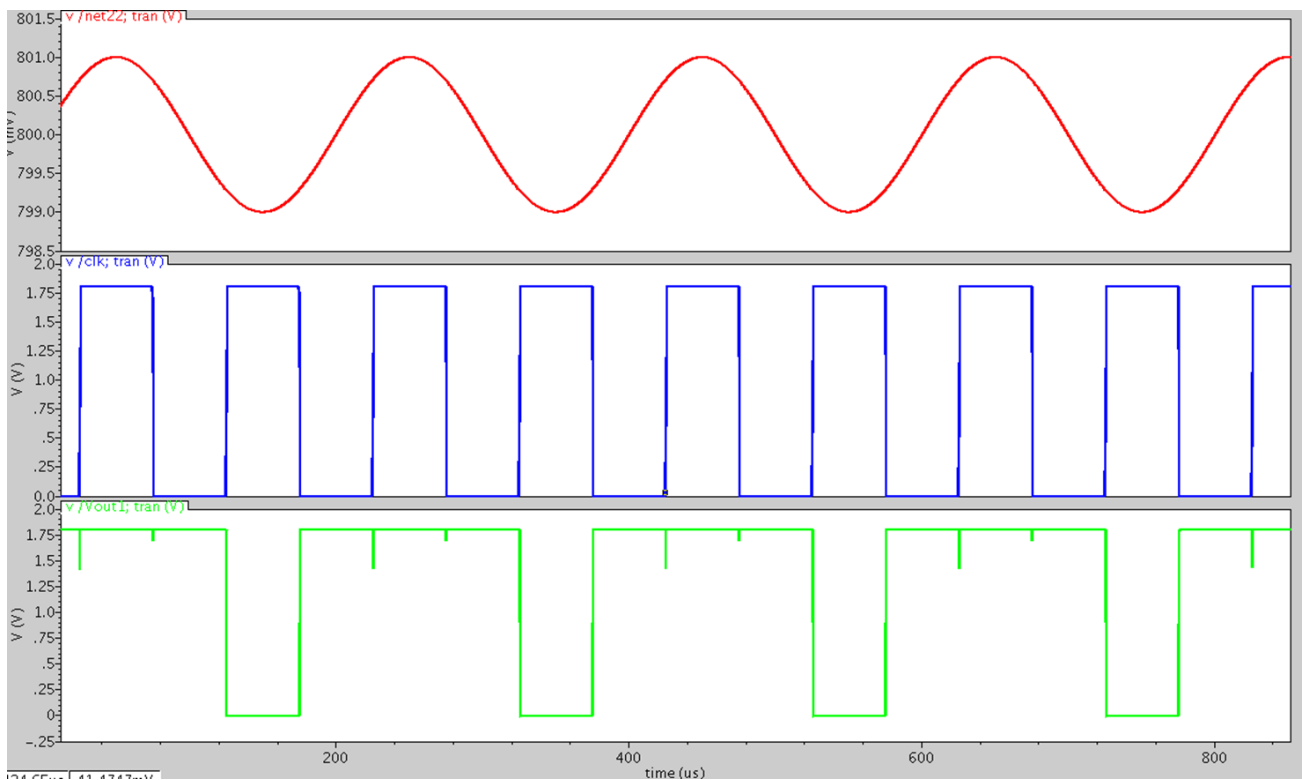


**Figure 30. Comparator Functionality**

This comparator circuit consumes 237nW of power, which fits our team’s purpose of building an ultra-low power transceiver.

## Complete Receiver Chain

The schematic for the complete receiver chain, which consists of the oscillator, the envelope detector, and the comparator, is shown in [Figure 31](#).

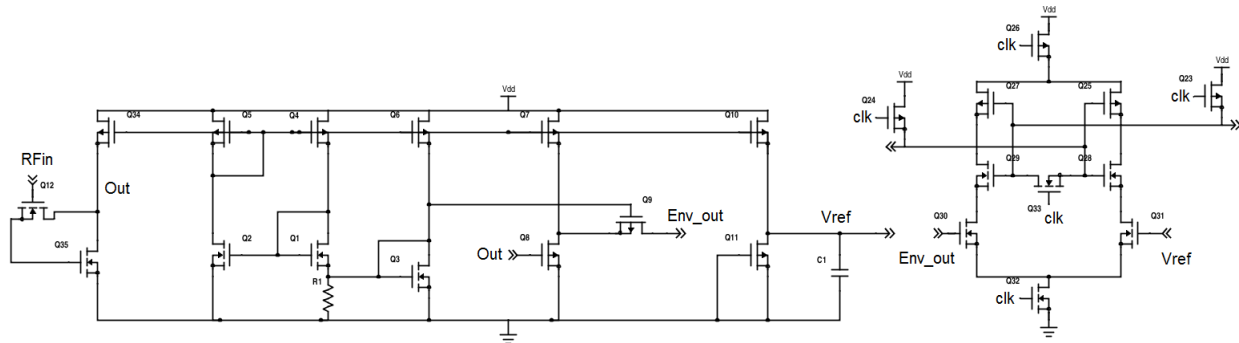


**Figure 31. Receiver Chain**

The capstone team verified the functionality of the receiver chain by inputting a test 1010 signal that is generated by the oscillator. The results of the simulation are shown in [Figure 32](#). As shown, the green signal is the generated 1010 signal from the oscillator. The purple square wave is the output of the envelope detector and as expected, it is the negative envelope of the input oscillator signal. The dc purple signal represents the reference voltage that the comparator uses to determine the received bits. For envelope amplitudes below the reference level, the comparator will clock a 1 and for envelope amplitudes above the reference level, the comparator will clock a 0. The red signal represents the clock signal. The blue signal represents the output of the comparator. An output synchronous flip flop that is edge triggered by the clock shown will latch a 1010, as expected.

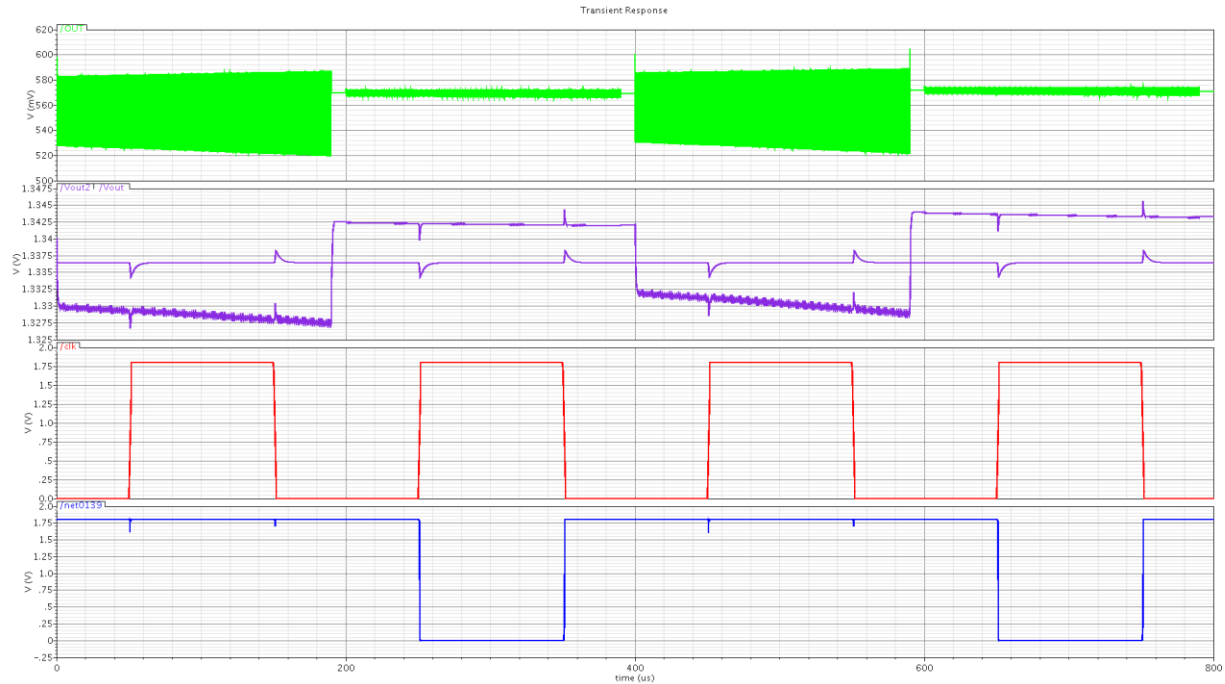


**Figure 32. Verification of Receiver**

## Power Amplifier

This part of the paper summarizes the design of a Power amplifier (PA) for the transmitter part of the system. This block functions to establish connections and send information from the digital system to the external world.

Given the fact that reducing the power consumption is the overall goal of this project, the power consumed by the individual blocks must also be minimized. This translates to the concept of power efficiency, meaning ‘the amount of power used to generate and transmit a decodable burst of data from the system’. The major trade off for efficiency is a characteristic called linearity.

Linearity defines ‘the relationship between the output and the input, and the change in output for

a given change in the input level'. Below is a table of the performance statistics of each of the power amplifier classes available.

CLASS	A	B	C	D	E
Theoretical efficiency	50%	78.5%	80%	100%	100%
Linearity	Linear	Non-linear	Non-linear	Non-linear	Non-linear

Since efficiency is our major consideration in this system, a class D amplifier was used. This choice was made after surveying highly efficient PA's in papers written in [32] and [33]. The other requirements needed for proper operation of the PA block include current bias generation, voltage bias at the input, and inclusion of passives.

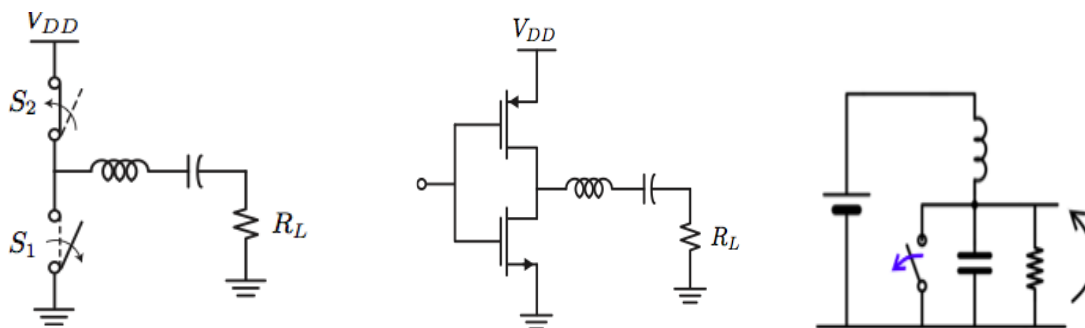
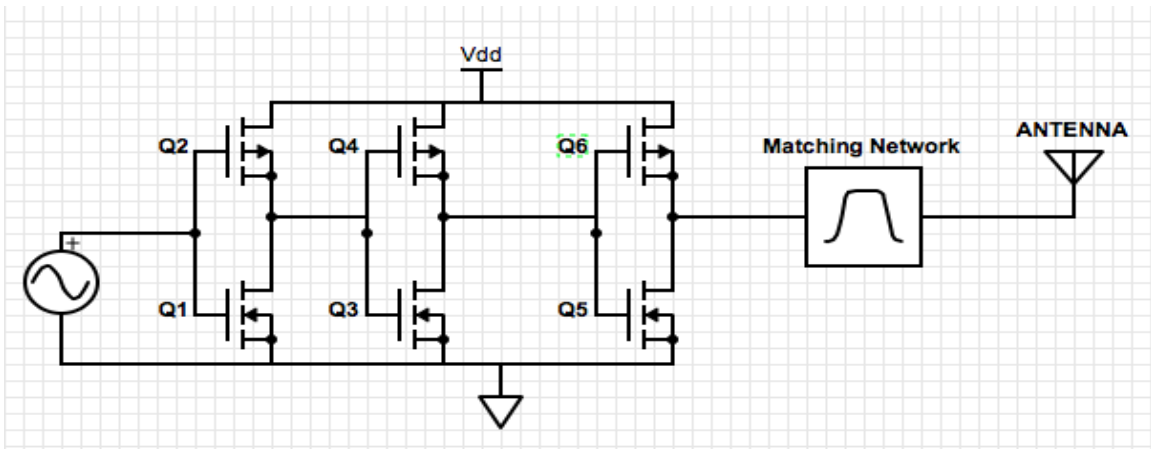


Figure 33. Class D & E Amplifier models [34]

From the above table, class D and class E amplifiers can be theoretically characterized as having an efficiency of 100% [34], this is because they don't allow for any dissipation of energy within the system, thus translating all of its energy to the required output load, which is an antenna used for transmission in most cases.



**Figure 34. Architecture of the Power Amplifier**

The control over power transmitted to the load depends on the impedance (resistance) of the load seen by the output node of the amplifier. In order to meet the specification of the power drawn by the load precisely, this load seen by the output node has to be transformed to a different value. This process of transforming the load can be done by using a network called ‘matching network’ to match the output node to the impedance needed for maximum power transfer. For this power amplifier, a T-match was employed because it isolates the DC component and the AC component – which is of our interest at the output node and also provides the impedance transformation needed. The final schematic of the power amplifier is shown in Figure 35.

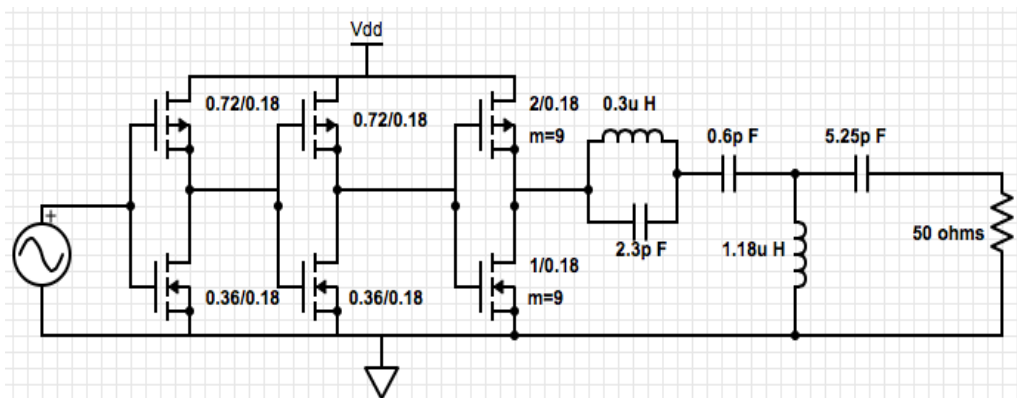


**Figure 35. Power Amplifier Schematic**

The layout of the power amplifier is shown in Figure 36.

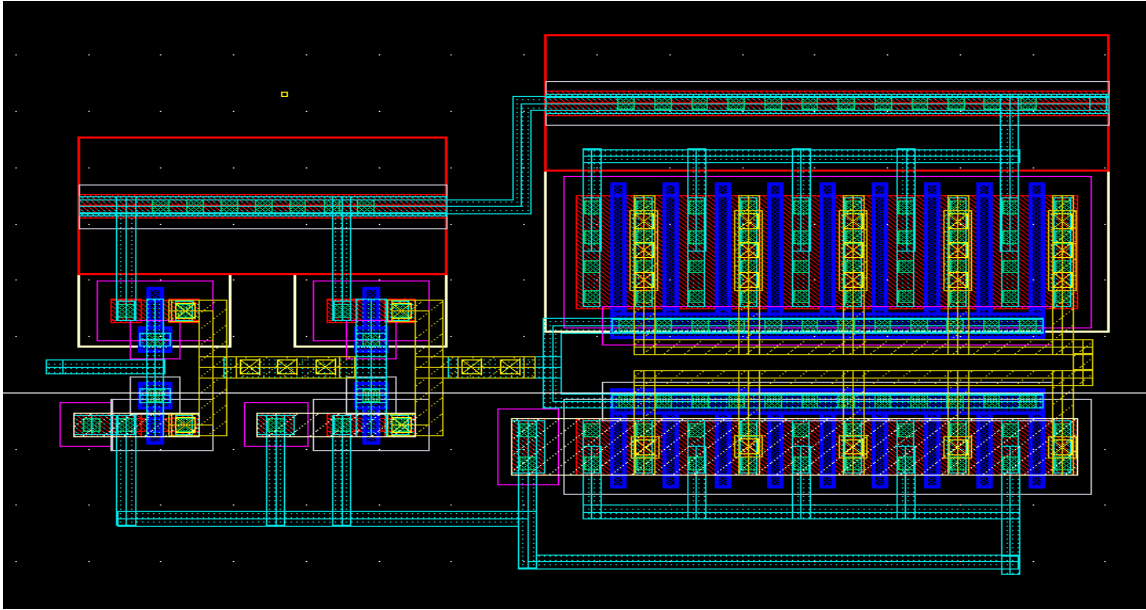


Figure 36. Power Amplifier Layout

The reported power gain is 47 dB at the fundamental frequency. The reported efficiency is 86.35% as shown in Figure 37.

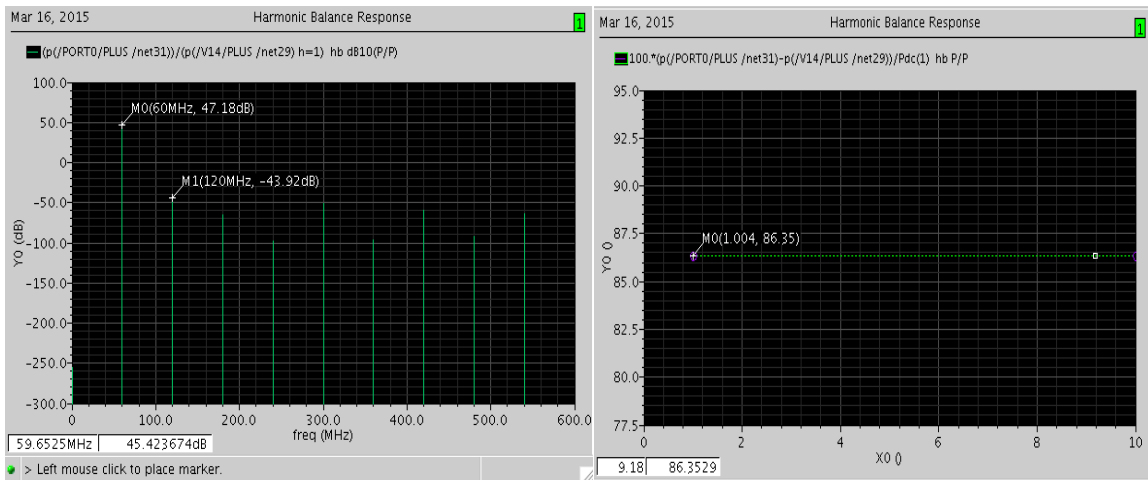
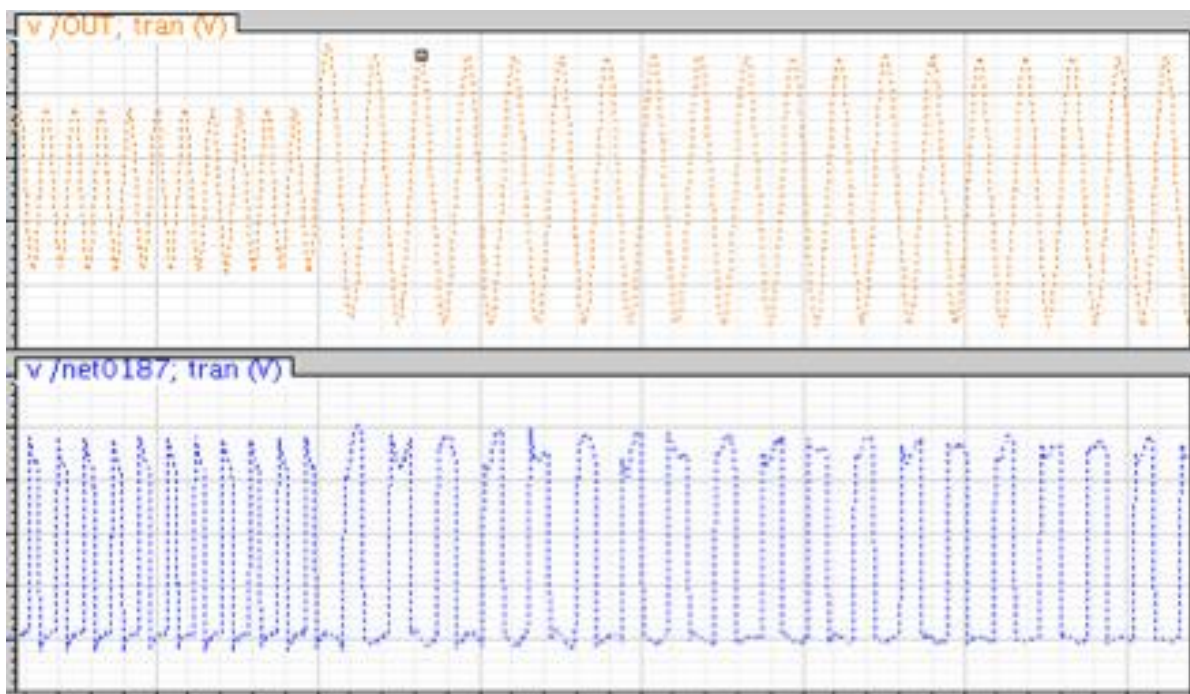


Figure 37. Measured Power Gain & Efficiency

## Transmit Chain

The oscillator is integrated with the Power amplifier by connecting the output of the oscillator to the input of the PA. An input FSK is generated by the oscillator and given to the PA.

The plot below shows how an input data stream is modulated and transmitted by the power amplifier into the antenna.



**Figure 38. Transmit Waveform**

## Voltage Buffer

The design requires a voltage buffer to interface with the  $50\Omega$  transmission line required to test our chip. This voltage buffer has several design requirements. The most important is a voltage gain of 1 to accurately represent the input signal. Impedance matching at the output is necessary to ensure that the maximum available power from the input signal is delivered to the load. The buffer also requires high enough bandwidth, output voltage swing, and linearity to send signals to the output negligible distortion. The input signals of interest are a 60MHz signal centered at 600mV with 0.8V peak to peak (pk-pk) and a 5kHz signal with 1.8Vpk-pk. A bandwidth requirement of 600MHz is necessary to capture harmonics of the 60MHz signal. Additionally, the buffer will connect a separate power rail from the rest of the transceiver to negate its power contribution during normal operation of the MEMS transceiver.

Given the design requirements presented, two separate buffers were implemented. A wideband buffer was designed for the 60MHz signal, while a rail-to-rail buffer was designed for the 5kHz signal. There exist a variety of different approaches to implement voltage buffers. Many single-stage amplifiers are described in the literature [35] [36] [37] [38]. These topologies are desired over op-amp based approaches mainly for their design simplicity and potential savings in die area and power consumption. However, their main disadvantage is the inability to reach the theoretical voltage gain of 1. Therefore, these topologies were not considered.

A different approach relies on tying an op amp into unity-gain feedback to set the voltage gain to 1. This feedback also decreases the output resistance by approximately the open-loop gain of the op amp, which further favors the conditions of an ideal voltage buffer. To properly send the large



input signals for our application, the op amp needs to have a large enough input common mode and output voltage swing. The op amp must also have the capability to drive low impedances, which requires the implementation of an output stage. For temperature independence, we also require a temperature independent current reference. The design of this reference is taken from [39] and is shown in [Figure 39](#).

The design of the wideband op-amp for the 60Mhz signal is shown in [Figure 40](#). The three stage op-amp topology consists of an input differential stage followed by a gain stage and an output stage. A series resistor and capacitor are used to increase stability in unity-gain feedback by moving the right half plane zero on top of the second pole. The output stage consists of a common source PMOS transistor, allowing the output to swing up to  $V_{dd}-V_{ov}$ . By contrast, if a source follower was used, the output could only swing up to  $V_{dd}-(V_{gs}+V_{ov})$ . Since our 60Mhz signal needs to swing up to 1V and  $V_{gs}+V_{ov} > 800\text{mV}$ , the source follower output stage would not have suited our application. The output stage resembles a push-pull inverter, but only the PMOS half is needed since we do not swing below 0V.

The output of our op amp in [Figure 40](#) shows the approach that is taken toward the impedance matching problem. The weakness of our unity gain feedback configuration is that the output resistance is not a clearly defined value. We can remedy this by adding an off-chip  $50\Omega$  resistor in series to have a matching impedance of about  $50\Omega$ , assuming that the op amp tied in feedback has a very low impedance. This systematically reduces the voltage gain by  $\frac{1}{2}$ , which is not detrimental since we can take this into account when viewing the waveform.

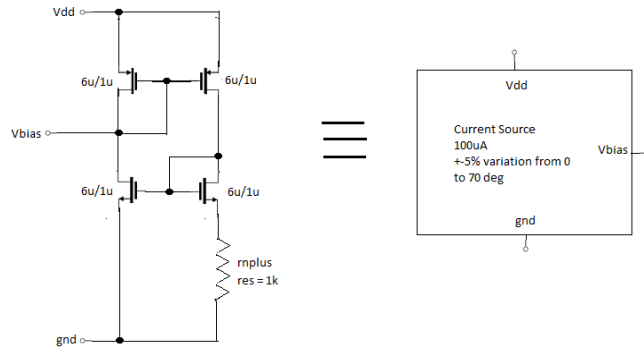


**Figure 39. Temperature Independent Current Reference**

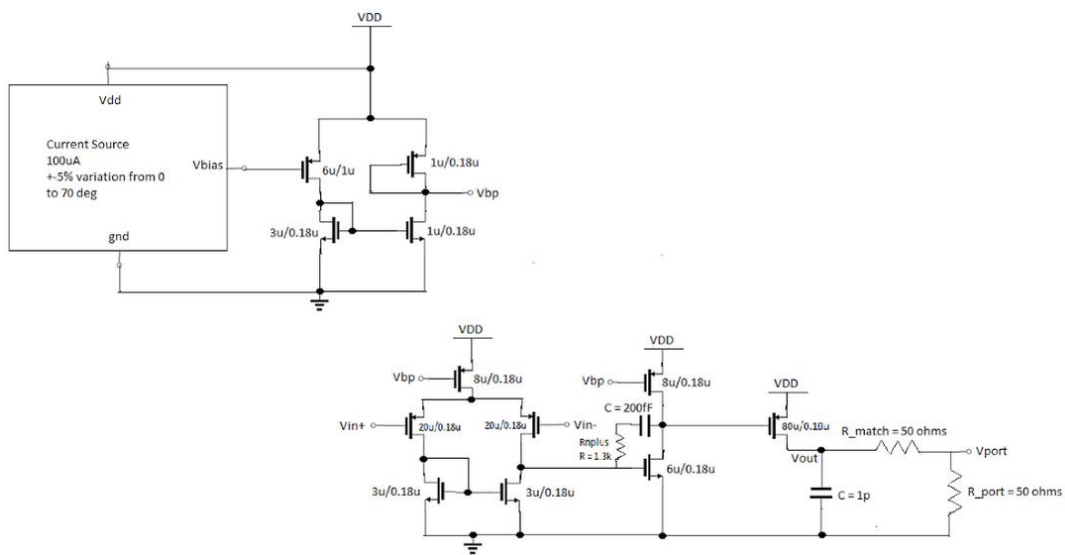


**Figure 40. Transistor-level Topology For Wideband Op-Amp**

The performance of the wideband op-amp is shown in [Figure 41](#). The transient response results with a 60Mhz 0.8Vpk-pk input signal also show negligibly small distortion. A tabulated summary of design specifications is given.

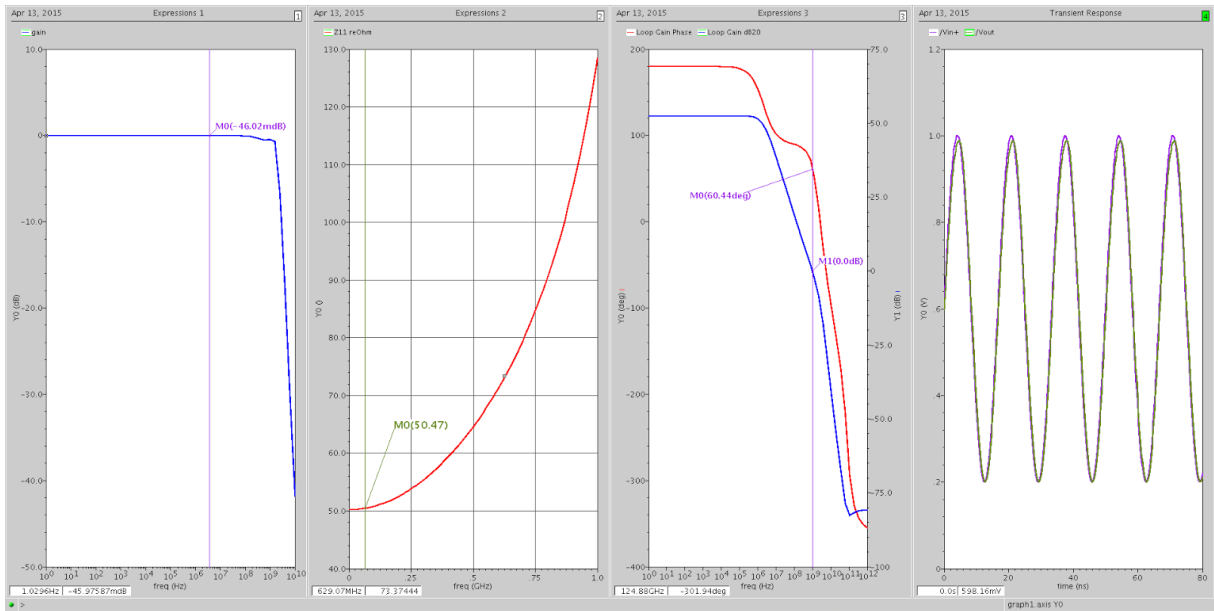
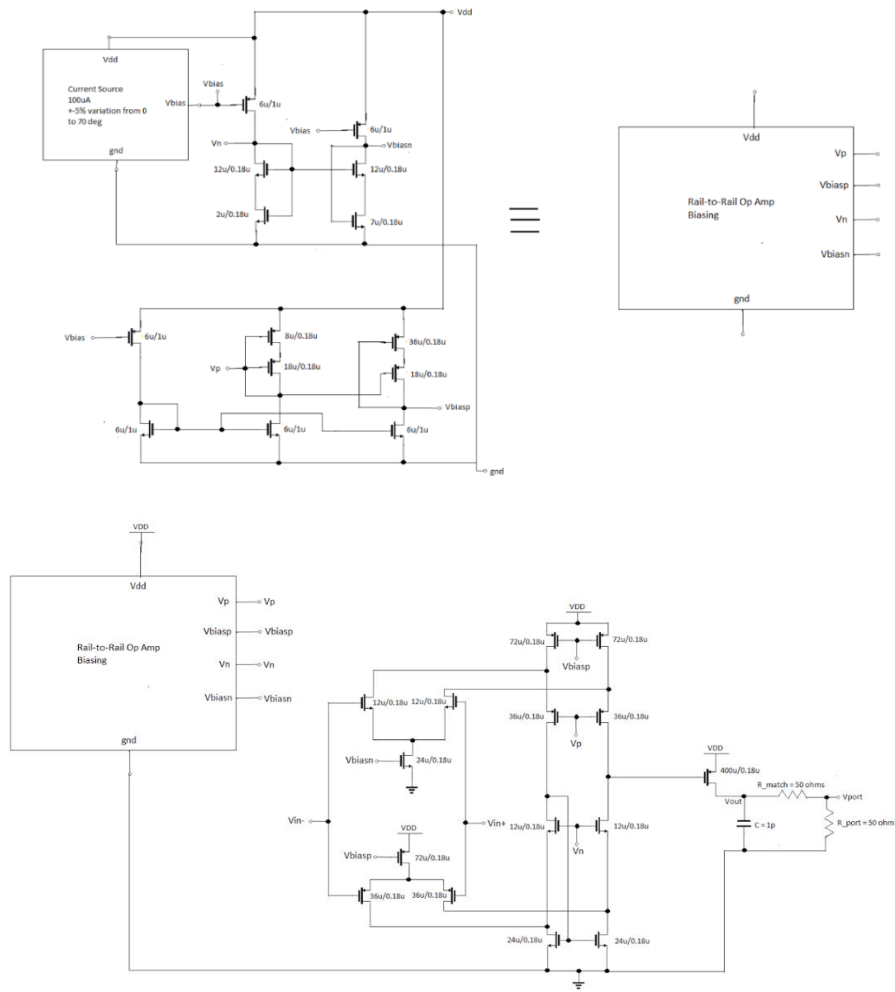


Figure 41. Wideband Op Amp Connected In Unity-gain Feedback

Design Spec	Wideband op-amp
DC Gain	1.0
3dB Bandwidth	1.9Ghz
1dB Av compression point (input signal DC level 600mV)	0.9V (Vpk-pk)
Total Power Consumption	12.4mW
Temperature Variations with I <sub>dc</sub>	+ - 5%
Output Impedance	50.44Ω at 60Mhz
Phase Margin	60.4 degrees
Frequency where loop gain is 0dB	1Ghz

The design of the rail-to-rail op-amp for the 5kHz signal is shown in [Figure 42](#) and replicates a design presented in [40]. An op-amp that can handle a rail-to-rail signal requires an input stage with a rail-to-rail common mode input range and an output stage with a rail-to-rail output swing. The input stage is a complementary differential pair with a cascoded load (Comp-Casc); it is

more easily recognizable as a combination of two folded cascode topologies. This input stage has common mode input range beyond both supply rails. The output stage is half of a push-pull inverter realized with common source transistors, similar to the wideband op amp.



**Figure 42. Transistor-level Topology Of The Rail-To-Rail Op Amp**

The resulting performance graphs of the rail-to-rail buffer can be seen in of [Figure 43](#). The buffer reaches the desired voltage gain and approximately the desired output impedance at 5khz. For the transient response, a 5khz rail-to-rail square wave was sent as the input. The maximum voltage of 1.67V results from needing to maintain a  $V_{ov}$  voltage drop across the PMOS output transistor and cannot be avoided by this topology. An additional off-chip 50Ω resistor is added at

the output for impedance matching. A tabulated summary of the performance for this buffer is shown.

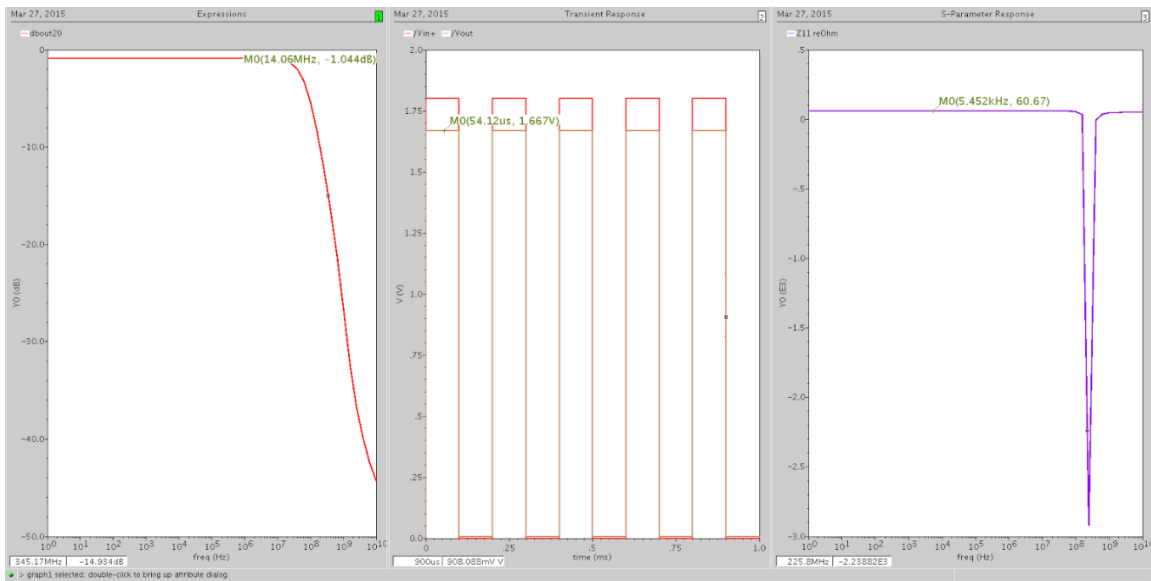


**Figure 43. Rail-To-Rail Op Amp Connected In Unity-gain Feedback.**

Design Spec	Wideband op-amp
DC Gain	1.0
1dB Bandwidth	14Mhz
Total Power Consumption	5.3mW
Temperature Variations with I <sub>dc</sub>	+ - 5%
Output Impedance	60.67Ω at 5khz
Phase Margin	~90 degrees
Frequency where loop gain is 0dB	60Mhz

## CONCLUSION

Our final prototype was designed using 180nm CMOS technology on Cadence, and the schematic was generated as part of this project. With the schematic of the system and layout of the oscillator/envelope detector complete, this transceiver system is almost ready for fabrication. However, the fabrication process usually takes several months and thus, this capstone team does not anticipate the opportunity of verifying the physical circuit. Despite this, we are confident in our simulation results and believe that the transceiver system designed in this project is functional and ready for applications.

The outcome discussed in this report reveals that it is possible to create a low power MEMS based transceiver. We successfully achieved our goal of designing a system that operates on 115 microwatts of power. In our market analysis, this capstone team identified many different applications for our technology and found that there is an immense need for low power transceiver systems in markets such as home, health, and agriculture. By successfully fulfilling our goals laid out in this capstone project, we have proven our hypothesis and we are excited to see where this technology is headed.

## WORKS CITED

- [1] Rocheleau, T., Naing, T., Nilchi, J., & Nguyen, C. (2014). A MEMS-BASED TUNABLE RF CHANNEL-SELECTING SUPER-REGENERATIVE TRANSCEIVER FOR WIRELESS SENSOR NODES. *Tech. Digest*, 83-86.
- [2] Nguyen, C. (2013, April 1). MEMS-Based RF Channel Selection for True Software-Defined Cognitive Radio and Low-Power Sensor Communications. *IEEE Communications Magazine*, 110-119.
- [3] Smith, P. (2011). Comparing Low-Power Wireless Technologies. Retrieved November 25, 2014. <http://www.digikey.com/en/articles/techzone/2011/aug/comparing-low-power-wireless-technologies>.
- [4] Dye, N., & Granberg, H. (2001). *Radio frequency transistors principles and practical applications* (2nd ed., p. 32). Boston: Newnes.
- [5] Lawson, S. (2014, November 18). ZigBee 3.0 promises one smart home standard for many uses. *PCWorld*.  
<http://www.pcworld.com/article/2849172/zigbee-30-promises-one-standard-for-many-uses.html>
- [6] Siekkinen, M., Hienkari, M., & Nurminen, J. (2012). How Low Energy is Bluetooth Low Energy? Comparative Measurements with ZigBee/802.15.4. *Embracing Machine-to-Machine Communications and Beyond*, 232-237. Retrieved from <http://www.eecs.umich.edu/courses/eecs589/papers/06215496.pdf>
- [7] Peiris, V. (2013). Highly integrated wireless sensing for body area network applications. *SPIE*, 1-3.
- [8] Hart, J., & Martinez, K. (2006, July 7). Environmental Sensor Networks: A revolution in the earth systems science? *Earth-Science Reviews*, 177-190.
- [9] Porter, M. (2008). The Five Competitive Forces that Shape Strategy. *Harvard Business Review*, 86-104, 431-452.
- [10] Sensors Value Chain. (2012). Retrieved February 13, 2015, from <http://gtq.imb-cnm.csic.es/en/about-us/sensors-value-chain>
- [11] Ulama, Darryle. (2014, December). IBISWorld Industry Report 33441a: Semiconductor and Circuit Manufacturing in the US. Retrieved February 13, 2015, from <http://clients1.ibisworld.com/reports/us/industry/default.aspx?indid=752>
- [12] Neville, A. (2014). IBISWorld Industry Report OD4422 Precision Agriculture Systems & Services. 3-26. Retrieved February 14, 2015, from [www.ibis.com](http://www.ibis.com)

- [13] Gerson, D. (2014, December 1). Smarter Food. Retrieved February 1, 2015, from [http://www.ibm.com/smarterplanet/us/en/food\\_technology/article/food\\_technology.html](http://www.ibm.com/smarterplanet/us/en/food_technology/article/food_technology.html)
- [14] Gainer, K. (2009). Environmental Sensing and Monitoring Technologies: Global Markets. (IAS030A), 1-1. Retrieved February 13, 2015, from <http://www.bccresearch.com/market-research/instrumentation-and-sensors/environmental-sensing-monitoring-ias030a.html>
- [15] American Farm Bureau Federation(2014). Fast fact about agriculture. Accessed February 14, 2015. from <http://www.fb.org/index.php?fuseaction=newsroom.fastfacts>
- [16] Southwire 2015 Distributor List Price Sheet: Copper Building Wire. <http://www.southwire.com/documents/pricesheets/466C.pdf>, accessed February 11, 2015.
- [17] Frenzel, Loue. "SDR And CR Boost Wireless Communications." *SDR And CR Boost Wireless Communications*. Electronic Design, 12 Oct. 2011. Web. 10 Mar. 2015. <<http://electronicdesign.com/dsps/sdr-and-cr-boost-wireless-communications>>.
- [18] Ismail, Sherille. "Transformative Choices: A Review of 70 Years of FCC Decisions." *Journal of Information Policy* 1 (2011): 6-35. Federal Communications Commission, 25 July 2014. Web.
- [19] Rocheleau, Tristan. "'A MEMS-based Tunable RF Channel-selecting Super-regenerative Transceiver for Wireless Sensor Nodes.'" *Solid-State Sensors, Actuators and Microsystems Workshop* (2014): n. pag. Web.
- [20] Lesurf, Jim. "The Envelope Detector." *The Envelope Detector*. University of St. Andrews, n.d. Web. 10 Mar. 2015. <[https://www.st-andrews.ac.uk/~www\\_pa/Scots\\_Guide/RadCom/part9/page2.html](https://www.st-andrews.ac.uk/~www_pa/Scots_Guide/RadCom/part9/page2.html)>.
- [21] Cha, Jeongwon. "A CMOS Radio-frequency Front-end for Multi-standard Wireless Communications." *A CMOS Radio-frequency Front-end for Multi-standard Wireless Communications*. Georgia Institute of Technology, 3 Mar. 2011. Web. 10 Mar. 2015. <<https://smartech.gatech.edu/handle/1853/37250?show=full>>.
- [22] Xia, Lingli. "Chapter 6." *Ultra Wideband RF Transceiver Design in CMOS Technology*. Intech, 2011. Web. 10 Mar. 2015. <<http://www.intechopen.com/books/ultra-wideband-communications-novel-trends-system-architecture-and-implementation/ultra-wideband-rf-transceiver-design-in-cmos-technology>>.
- [23] Lai, Xiongliang. "A Comparative Study of Low-power CMOS Gilbert Mixers in Weak and Strong Inversion." *IEEE Xplore*. Institute of Electrical and Electronic Engineers, 7 Aug. 2011. Web. 10 Mar. 2015.
- [24] Raab, F.h., P. Asbeck, S. Cripps, P.b. Kenington, Z.b. Popovic, N. Pothecary, J.f. Sevic, and N.o. Sokal. "Power Amplifiers and Transmitters for RF and Microwave." *IEEE Transactions on Microwave Theory and Techniques* 50.3 (2002): 814-26. Web.



- [25] Gambini, Simone. "Sensitivity Analysis for AM Detectors." *Sensitivity Analysis for AM Detectors*. UC Berkeley, 6 Apr. 2008. Web. 10 Mar. 2015. <<http://www.eecs.berkeley.edu/Pubs/TechRpts/2008/EECS-2008-31.html>>.
- [26] Zhou, Yanping. "A Novel Wide-band Envelope Detector." *IEEE Xplore*. N.p., 17 June 2008. Web. 10 Mar. 2015. <<http://ieeexplore.ieee.org/xpl/articleDetails.jsp?arnumber=4561422>>.
- [27] R.G. Meyer Low-power monolithic RF peak detector analysis *IEEE Journal of Solid-State Circuits*, January 1995.
- [28] D.C.Daly and A.Chandrakasan An energy efficient OOK transceiver for wireless sensor networks *IEEE Journal of Solid-state Circuits*, May 2007.
- [29] Pletcher, Nathan, Jan Rabaey, and Simone Gambini. "A 65uW, 1.9 GHz RF to Digital Baseband Wakeup Receiver for Wireless Sensor Nodes." *IEEE Xplore*. N.p., 16 Sept. 2007. Web. 10 Mar. 2015. <[http://ieeexplore.ieee.org/xpls/abs\\_all.jsp?arnumber=4405789](http://ieeexplore.ieee.org/xpls/abs_all.jsp?arnumber=4405789)>.
- [30] Alon, Elad. "EE240: Advanced Analog Integrated Circuits Lectures." *EE240 (Spring 2009)*. N.p., 2009. Web. 10 Mar. 2015. <[http://bwrce.eecs.berkeley.edu/Classes/icdesign/ee240\\_sp10/lectures.html](http://bwrce.eecs.berkeley.edu/Classes/icdesign/ee240_sp10/lectures.html)>.
- [31] Sanborn, Keith. "A Sub-1-V Low-Noise Bandgap Voltage Reference." *IEEE Xplore*. N.p., Nov. 2007. Web. 10 Mar. 2015. <<http://ieeexplore.ieee.org/stamp/stamp.jsp?arnumber=4362111>>.
- [32] Nathan o. sokal,(1981) ieee life fellow design automation, inc: Class-e high-efficiency rf/microwave power amplifiers: principles of operation, design procedures, and experimental verification retrieved February 1981 from: <http://www.cs.berkeley.edu/~culler/AIIT/papers/radio/Sokal%20AACD5-poweramps.pdf>
- [33] N.O.Sokal and A.D.Sokal (1975),“Class E—A new class of high-efficiency tuned single-ended switching power amplifiers,” *IEEE J. Solid-State Circuits*, vol. SC-10, no. 6, pp. 168–176, Jun. 1975. [http://ieeexplore.ieee.org/xpls/abs\\_all.jsp?arnumber=1050582](http://ieeexplore.ieee.org/xpls/abs_all.jsp?arnumber=1050582)
- [34] Ali.M.Niknejad (2014): RFIC ,UC Berkeley; EE242B, retrieved fall 2014 from: <http://rfic.eecs.berkeley.edu/ee242/lectures.html>
- [35] Aseem, J., Padaliya, J., & Savani, V. (2012). Analysis and Characterization of Different Voltage Follower Topologies in 90nm Technology. *International Journal of Emerging Technology and Advanced Engineering*, 2(12), 229-235.
- [36] Carvajal, R., Ramirez-Angulo, J., Lopez-Martin, A., Torralba, A., Galan, J., Carlosena, A., & Chavero, F. (2005). The Flipped Voltage Follower: A Useful Cell for Low-Voltage Low-Power Circuit Design. *IEEE Transactions on Circuits and Systems*, 52(7), 1276-1290.

- [37] Koutani, M., Fujimoto, Y., & Miyamoto, M. (2003). A Highly Linear CMOS Buffer Circuit with an Adjustable Output Impedance. *IEEE Custom Integrated Circuits Conference*, 685-688.
- [38] Shedge, D., Itole, D., Gajare, M., & Wani, P. (2013). Analysis and Design of CMOS Source Followers and Super Source Follower. *ACEEE Int J. on Control System and Instrumentation*, 2(4), 54-58.
- [39] Grey, P., Meyer, R., Hurst, P., & Lewis, S. (2009). *Analysis and Design of Analog Integrated Circuits* (5th ed.). John Wiley & Sons.
- [40] Lorenzo, M., Manzano, A., Gusad, M., Hizon, J., & Rosales, M. (2007). Design and Implementation of CMOS Rail-to-Rail Operational Amplifiers. *2007 International Symposium on Communications and Information Technologies*, 61-66.
- [41] Rocheleau, T., Naing, T., Nilchi, J., & Nguyen, C. (2014). A MEMS-Based Tunable RF Channel-Selecting Super-Regenerative Transceiver For Wireless Sensor Nodes. *2014 Hilton Head MEMS Conference*, 83-86.